Advances in Colloid and Interface Science 343 (2025) 103558

Contents lists available at ScienceDirect

Advances in Colloid and Interface Science

journal homepage: www.elsevier.com/locate/cis

Progress in silicon-based materials for emerging solar-powered green hydrogen (H_2) production

Aminul Islam [a,b,c,**], Md. Tarekul Islam [d], Siow Hwa Teo [e], Hasan Mahmud [f], A.M. Swaraz [g], Ariyan Islam Rehan [h], Adiba Islam Rasee [i], Khadiza Tul Kubra [i], Md. Munjur Hasan [i], Md. Shad Salman [j], R.M. Waliullah [j], Md. Nazmul Hasan [h], Md. Chanmiya Sheikh [k], Tetsuya Uchida [k], Mrs Eti Awual [i], Mohammed Sohrab Hossain [i], Hussein Znad [l], Md. Rabiul Awual [l,*]

[a] *Department of Petroleum and Mining Engineering, Jashore University of Science and Technology, Jashore 7408, Bangladesh*
[b] *Hydrogen energy and CO_2 conversion Lab, Department of Petroleum and Mining Engineering, Jashore University of Science and Technology, Jashore 7408, Bangladesh*
[c] *College of Engineering, Korea University, 145 Anam-ro, Seongbuk-gu, Seoul 02841, Republic of Korea*
[d] *Department of Leather Engineering, Faculty of Mechanical Engineering, Khulna University of Engineering and Technology, Khulna 9203, Bangladesh*
[e] *Industrial Chemistry Program, Faculty of Science and Natural Resources, Universiti Malaysia Sabah, 88400 Kota Kinabalu, Sabah, Malaysia*
[f] *Bangladesh Energy and Power Research Council (BEPRC), IEB Bhaban (11th Floor), Ramna, Dhaka 1000, Bangladesh*
[g] *Department of Genetic Engineering and Biotechnology, Jashore University of Science and Technology, Jashore, 7408, Bangladesh*
[h] *Department of Chemistry, School of Science, The University of Tokyo, 7-3-1 Bunkyo-ku, Tokyo 113-0033, Japan*
[i] *Department of Chemistry, Graduate School of Science, Osaka University, Osaka 560-0043, Japan*
[j] *Institute for Chemical Research, Kyoto University, Gokasho, Uji, Kyoto 611-0011, Japan*
[k] *Division of Applied Chemistry, Graduate School of Natural Science and Technology, Okayama University, 1-1 Tsushima-naka, 3-Chome, Okayama 700-8530, Japan*
[l] *Western Australian School of Mines: Minerals, Energy and Chemical Engineering, Curtin University, GPO Box U 1987, Perth, WA 6845, Australia*

ARTICLE INFO

Keywords:
Silicon-based materials
Water splitting
Hydrogen
Sustainable
Clean and renewable energy

ABSTRACT

The imperative demand for sustainable and renewable energy solutions has precipitated profound scientific investigations into photocatalysts designed for the processes of water splitting and hydrogen fuel generation. The abundance, low toxicity, high conductivity, and cost-effectiveness of silicon-based compounds make them attractive candidates for hydrogen production, driving ongoing research and technological advancements. Developing an effective synthesis method that is simple, economically feasible, and environmentally friendly is crucial for the widespread implementation of silicon-based heterojunctions for sustainable hydrogen production. Balancing the performance benefits with the economic and environmental considerations is a key challenge in the development of these systems. The specific performance of each catalyst type can vary depending on the synthesis method, surface modifications, catalyst loading, and reaction conditions. The confluence of high crystallinity, reduced oxygen concentration, and calcination temperature within the silicon nanoparticle has significantly contributed to its noteworthy hydrogen evolution rate. This review provides an up-to-date evaluation of Si-based photocatalysts, summarizing recent developments, guiding future research directions, and identifying areas that require further investigation. By combining theoretical insights and experimental findings, this review offers a comprehensive understanding of Si-based photocatalysts for water splitting. Through a comprehensive analysis, it aims to elucidate existing knowledge gaps and inspire future research directions towards optimized photocatalytic performance and scalability, ultimately contributing to the realization of sustainable hydrogen generation.

---

* Corresponding author. Western Australian School of Mines, Minerals, Energy and Chemical Engineering, Curtin University, GPO Box U 1987, Perth, WA, 6845, Australia.

** Corresponding author at: Department of Petroleum and Mining Engineering, Jashore University of Science and Technology, Jashore 7408, Bangladesh.

E-mail addresses: aminul_pme@just.edu.bd (A. Islam), adiba.islam@dims-bd.org (A.I. Rasee), munjur.hasan@dims-bd.org (Md.M. Hasan), r.waliullah@dims-bd.org (R.M. Waliullah), chanmiya.sheikh@dims-bd.org (Md.C. Sheikh), sohrab.hossain@dims-bd.org (M.S. Hossain), rabiul.awual@dims-bd.org, rawual76@yahoo.com, rabiul.awual@curtin.edu.au (Md.R. Awual).

https://doi.org/10.1016/j.cis.2025.103558
Received in revised form 1 May 2025;
Available online 27 May 2025

1. Introduction

The importance of hydrogen as a potential green energy source is rising. Its importance stems from its ability to alleviate a variety of environmental concerns and resource depletion associated with the current reliance on fossil fuels. Additionally, hydrogen has significant value as a chemical feedstock and finds applications in industries such as petrochemicals and ammonia synthesis. Currently, the industrial production of hydrogen primarily relies on three main processes: steam-methane reforming, coal gasification, and water splitting. However, the first two methods heavily rely on fossil fuels and result in substantial CO_2 emissions, contributing to climate change. In contrast, water splitting offers a promising and environmentally responsible approach to hydrogen production. Water splitting involves the separation of water molecules into hydrogen and oxygen using various methods. With water being abundant on Earth, the utilization of water splitting as a method for environmentally friendly hydrogen production becomes highly desirable. Moreover, the renewable nature of hydrogen reinforces its sustainability as a green energy alternative.

Silicon, as a semiconductor material, possesses several advantageous properties that make it widely used in photovoltaic devices. The material's broad light absorption across the solar spectrum, coupled with its Earth-abundant and low charge carrier recombination rate, renders it highly effective for solar energy conversion. Integration of p-n silicon junctions with water splitting technology facilitates direct capture and conversion of solar energy into hydrogen fuel. This approach exhibits particular promise for decentralized power generation and storage due to its suitability for small-scale solar-to-fuel devices [1]. The combination of solar energy capture and conversion with water splitting in a single device can improve efficiency, reduce costs, and enhance the practicality of solar-to-fuel technologies. Moreover, the use of silicon, which is abundant and cost-effective compared to noble metals, makes this integrated approach more commercially viable [2]. It opens up possibilities for scaling up the production of solar-to-fuel devices and facilitating their widespread adoption in various applications.

In silicon, at room temperature, all electrons reside in the valence band, leaving the conduction band empty. This electronic configuration renders silicon an insulator, as no free electrons are available to conduct electricity. External energy sources, such as light or heat, can induce electronic excitation within a material. Specifically, light can trigger the promotion of electrons from the valence to the conduction band through a process known as photoexcitation. Similarly, thermal energy can facilitate the same transition via thermal excitation [3]. This absorption of energy elevates the electrons to higher energy levels within the conduction band, transforming them into free charge carriers capable of movement within the silicon lattice. This movement constitutes electrical conductivity, effectively transforming the once insulating silicon into a semiconductor [3]. Silicon's ability to exhibit this behavior makes it a crucial material in the field of electronics. It is widely used to create semiconductors, such as computer chips, where the controlled movement of electrons is essential for various electronic functions. Due to its narrow band gap (around 1.12 eV for silicon), silicon exhibits excellent optical absorption properties, particularly in the visible light spectrum [4]. Many researchers have been working on designing and developing architectures and materials that utilize silicon as a semiconductor in photocatalytic systems [3,4]. This area of research holds promise for advancing sustainable and clean energy production using silicon-based photocatalytic systems for hydrogen fuel generation.

The ability to engineer the bandgap of semiconductor materials and develop nanostructured photocatalysts has opened significant possibilities for efficient solar-active materials. The successful conversion of solar energy into hydrogen via photocatalytic water splitting is highly dependent on the physicochemical properties and photocatalytic activity of the chosen photocatalyst material. This dependence arises from the fact that these properties directly influence the material's ability to absorb light, generate charge carriers, and facilitate the water-splitting reactions at its surface [5]. In addition to the design of efficient nanostructured photocatalysts, the exploration of co-catalysts is another important area of research in this field. Co-catalysts are materials that can enhance the efficiency of photocatalytic reactions, thus improving the overall performance of the system. Identifying cost-effective, stable, and scalable co-catalysts is crucial for practical applications of solar-driven water splitting [5]. The surface of silicon can be functionalized with various co-catalyst nanoparticles, enhancing its catalytic activity and efficiency in wastewater-splitting actions. Furthermore, nanostructured silicon, including silicon nanowires, black silicon, silicon nanosheets, and silicon carbide or nitride, along with their composite heterojunctions, are considered highly promising materials for generating hydrogen through water splitting.

Bandgap engineering in semiconductor materials is a key factor in achieving high-energy conversion efficiency in photocatalytic reactions. By carefully tuning the bandgap of a semiconductor to match the solar spectrum, more photons can be effectively absorbed, leading to enhanced light utilization and higher energy conversion rates. Techniques such as doping and the formation of multi-junction heterostructures have opened possibilities for tailoring the bandgaps of semiconductor materials. Nanostructured semiconductor photocatalysts have gained significant attention due to their improved light absorption properties and the ability to facilitate solar-driven catalytic reactions. These nanostructured materials offer enhanced surface area and unique structural features, which enable better light absorption and efficient catalytic reactions.

Limited activity on silicon surfaces creates opportunities for diverse nanoparticles to bind, leading to enhanced photocatalysis and selective product formation in water splitting [6]. Compared to bulk silicon, nanoparticles exhibit enhanced reactivity and can generate hydrogen more rapidly [6]. Various nanostructured forms of silicon, such as silicon nanowires, black silicon, silicon nanosheets, and silicon carbide or nitride, have shown promise as materials for generating hydrogen through water splitting. Composite heterojunctions, characterized by the intimate integration of distinct nanostructured materials, stand out as highly promising candidates for driving efficient solar-driven water splitting.

To highlight recent developments, lingering issues, and potential progress, a cutting-edge evaluation of the connection of diverse nanostructured silicon photocatalysts is essential. To protect the environment, it is important to compare current, cutting-edge technologies. There aren't many review papers available on this topic. Researchers [7,8] have reported on a sustainable photocatalytic method for producing hydrogen from water with an emphasis on photocatalytic hydrogen generation employing homogeneous, heterogeneous, and hybrid systems catalysts. Reviews on the Various treatment methods for enhanced bio-hydrogen production have been published [9,10]. Some attention has been paid to solid-state hydrogen storage and Green Fuels production [11,12].

The potential of silicon carbide (SiC) for photoelectrochemical (PEC) H_2 production has undergone thorough investigation in recent years, with significant progress being documented. This exploration has focused on understanding and optimizing the various factors that influence SiC's performance in this application. These efforts aim to harness the unique properties of SiC, such as its suitable bandgap, excellent chemical stability, and high durability, for efficient sunlight-to-hydrogen conversion [13,14]. An approach to produce high-performance hydrogen by tuning band gap and surface functional groups was highlighted by several researchers [15–19]. Recent research has extensively explored the application of black-silicon-assisted photovoltaic cells for achieving higher conversion efficiencies. These studies have not only highlighted the opportunities afforded by the nanotextured surface of black silicon in enhancing light trapping and reducing reflectance, but also critically evaluated the challenges associated with its fabrication processes [20,21]. Recently, Semiconductor based nanomaterial photocatalysts are acquiring expanding perceptible for hydrogen production through water-splitting [22,23]. Consequently, the exploration of nanostructured silicon photocatalysts for water splitting has constituted a focal point of ongoing research endeavors. Nevertheless, a limited review has been paid attention to wireless solar green hydrogen production with nanostructured silicon photocatalysts.

A comprehensive overview of recent developments in silicon photocatalysts for water-splitting-driven hydrogen production is presented in the review. This summary highlights the key advancements achieved in this field, focusing on various strategies employed to enhance the photocatalytic performance of silicon for efficient hydrogen generation. The various types of nanostructured silicon materials, such as silicon nanowires, black silicon, silicon nanosheets, and composite heterojunctions, and their performance as photocatalysts have been discussed. Furthermore, the theoretical approaches used to understand and optimize the properties and performances of these silicon photocatalysts have been highlighted. It combines experimental findings, theoretical insights, and general information to provide a holistic understanding of the field and contribute to the progress in sustainable hydrogen production through solar-driven water splitting.

2. Mechanistic understanding of silicon photocatalyst

Semiconductor-based photocatalysis has garnered significant research interest due to its potential for clean and sustainable solar-driven water splitting, a process that converts sunlight and water into hydrogen fuel. Elucidating the intricate mechanisms governing this water-to-fuel transformation is critical for optimizing photocatalyst performance and unlocking its full potential. A significant obstacle in the field of photoelectrochemical water splitting remains the attainment of unassisted water splitting. This refers to a process where both the hydrogen evolution reaction (HER) and oxygen evolution reaction (OER) occur spontaneously, without requiring an external electrical bias. Thermodynamically, this process necessitates a minimum bandgap potential of approximately 1.7–1.8 V to overcome the inherent water molecule stability. Water splitting has a 1.23 V thermodynamic potential at 20 °C. The photocatalytic water-splitting mechanism [24] is depicted in Fig. 1. The process entails the catalyst's excitation by the absorption of light, wherein the absorbed light energy must be equivalent to or surpass the band gap of the semiconductor material comprising the catalyst. Upon excitation, an electron is promoted from the valence to the conduction band of the semiconductor, creating a corresponding hole in the vacated valence band. These photogenerated electron-hole pairs serve as the driving force for the subsequent chemical reactions. Following the absorption of light energy exceeding the band gap of the semiconductor material, the excited catalyst undergoes the subsequent liberation of charge carriers. The liberation process triggered by light absorption in semiconductors leads to the dissociation of the initially formed bound electron-hole pairs. This phenomenon results in the generation of free electrons within the conduction band and holes within the valence band, paving the way for their participation in subsequent photocatalytic reactions. In instances where the excitation energy significantly surpasses the band gap energy (Eg), the excess energy may lead to the occupation of energy sub-bands. For excited holes, these sub-bands are situated below the valence band maximum (VBM), while for excited electrons, they are positioned above the conduction band minimum (CBM). According to Ahmed et al. [24], the following equations can explain how the extra energy is distributed:

$$\Delta E_e = \left(h\nu - E_g\right)\left[1 + {m_e}^{*}/{m_h}^{*}\right]^{-1} \tag{1}$$

$$\Delta E_h = \left(h\nu - E_g\right) - \Delta E_\mathrm{e} \tag{2}$$

The presented equations illuminate the energetic landscape of photocatalysis, unraveling the distribution and utilization of excess energy within the semiconductor material. These equations, where $m_e{}^*$ and $m_h{}^*$ represent the effective masses of electrons and holes, respectively, and ΔE_e and ΔE_h signify the energy differences between photogenerated carriers and their respective band edges, demystify the intricate workings of photocatalysis, paving the way for breakthrough advancements. The presented equations afford insights into the distribution and utilization of excess energy within the semiconductor material during photocatalytic processes, thereby influencing the overall efficiency and performance of the photocatalyst. Delving into the dynamics of charge carriers and the intricacies of energy distribution within a semiconductor photocatalyst proves indispensable for garnering profound insights into the underlying mechanisms governing its function. These insights serve as invaluable guiding principles for meticulously optimizing the design of such photocatalysts, ultimately leading to enhanced efficiency in water-splitting applications. The possible mechanism of

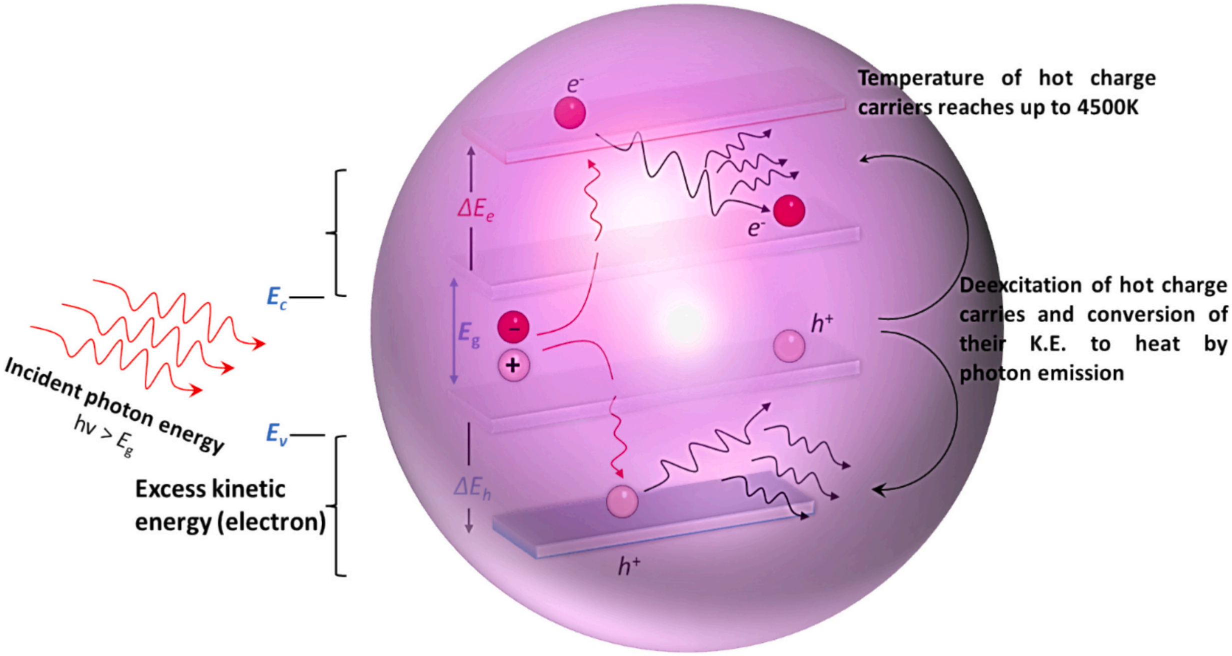

Fig. 1. The mechanism of photocatalysis under light irradiation.

silicon (Si)-initiated water splitting on the smallest unit of silicon, indicates that the process does not follow the conventional pathway of water splitting [25]. Hydrosilylation stands in contrast to conventional hydrogenation reactions, as it hinges on a distinct mechanism. This mechanism revolves around the fragmentation of Si—H bonds, followed by the concurrent formation of Si-OH bonds, leading to the desired product formation. This transformation signifies the replacement of a hydrogen atom with a hydroxyl group on the silicon center. This mechanistic process is elucidated in Fig. 2. As outlined in the investigation conducted by Liu et al. [25], pristine Si nanowires predominantly engage in the subsequent reactions attributable to the existence of Si—H bonds:

$$Si(h^{+}) + Si - H(e-) + H_2O\ Si - OH + Si + H_2 \tag{3}$$

In this reaction, Si(h+) represents a positively charged silicon species, Si-H(e-) represents an electron in a Si—H bond, and Si-OH, Si, and H_2 are the resulting products [25]. Heterolytic cleavage of Si—H bonds on the surface of the material, followed by the subsequent formation of Si-OH bonds, constitutes a key activation pathway for H_2 gas production, leading to a significantly higher probability of H_2 generation compared to O_2 evolution.

It is important to consider the interactions between oxygen species and the catalyst surface [25]. The process involves the formation of hydroxyl (OH^-) and superoxide (O^2) radicals. The electron-deficient H atoms on the Si surface are believed to act as electron acceptors, facilitating efficient charge separation by capturing electrons from photogenerated electron-hole pairs. These strategies may include electrochemical reduction, carbothermal reduction, self-templating synthesis, and magnetiothermic reduction. These techniques enable the synthesis of nanomaterials with desired properties and structures for efficient photocatalytic water splitting.

A mechanistic understanding of silicon-based photocatalysts has been extensively explored due to their promising potential in facilitating efficient solar-driven water splitting for sustainable hydrogen production. The fundamental principle underlying semiconductor photocatalysis involves the absorption of photons with energy equal to or exceeding the band gap (Eg) of the semiconductor, resulting in the excitation of electrons from the valence band to the conduction band and the simultaneous generation of holes. These photogenerated charge carriers act as the primary agents driving redox reactions on the catalyst surface. A critical requirement for unassisted water splitting is a minimum bandgap potential of approximately 1.7–1.8 V, which is necessary to overcome the inherent stability of water molecules, despite the thermodynamic potential for water splitting being only 1.23 V at 20 °C. Notably, silicon exhibits a unique mechanistic pathway distinct from conventional semiconductor-mediated water splitting. This alternative pathway involves the heterolytic cleavage of surface Si—H bonds and their transformation into Si-OH species in the presence of water. This process, often referred to as hydrosilylation, results in the generation of molecular hydrogen while circumventing the traditional HER-OER pathway. The photogenerated holes localized on the silicon surface are thought to facilitate this bond cleavage, thereby enhancing hydrogen evolution. Furthermore, the interaction between oxygen species and the silicon surface contributes to efficient charge separation through the formation of OH^- and O_2^- radicals, thereby suppressing recombination losses. These findings underscore the need for tailoring nanostructured Si-based photocatalysts through advanced synthesis techniques such as carbothermal and magnetiothermic reduction to optimize their structural and electronic properties for enhanced catalytic activity.

3. Approaches and advances of silicon photocatalyst synthesis

Si-based photocatalysts typically consist of silicon (Si) as the main component and are modified with various functional groups or dopants

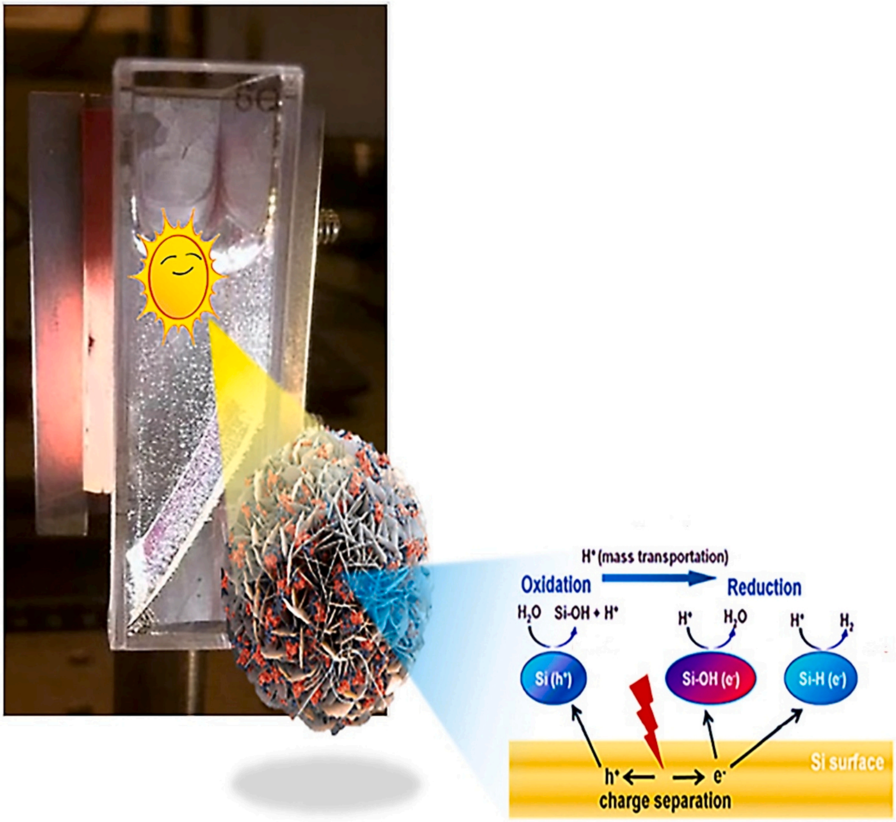

Fig. 2. The mechanistic approach of H_2 production over silicon photocatalyst.

to enhance their photocatalytic activity. The morphological aspects of Si, such as shape, size, geometry, and crystal phases, directly impact photocatalytic activity [26]. These parameters can affect the availability of surface-active sites, electron transport, and mass transfer within the photocatalyst. Various morphologies of Si have been explored, including microspheres, nanospheres, nanosheets, nanorods, nanotubes, and nanowires. Each morphology offers unique properties and advantages for photocatalytic applications. In addition to morphology, the presence of impurities in Si-based photocatalysts also plays a significant role in their design [27]. Impurities can have a notable impact on the optical properties of silicon and can be deliberately introduced to modulate its photocatalytic behavior. The incorporation of specific impurities can alter the band structure, charge carrier dynamics, and surface properties of Si, thereby enhancing its photocatalytic performance. It is worth noting that the production of pure silicon from silica (silicon dioxide) through reduction requires considerable time and energy. This phenomenon is predominantly attributed to the elevated bonding energy existing between silicon and oxygen atoms within silica [27]. Different routes to produce silicon from silica [28,29] are shown in Fig. 3. However, advancements in synthesis techniques have enabled the fabrication of Si-based photocatalysts with controlled impurity levels and improved optical properties, making them suitable for photocatalytic applications.

The synthesis of silicon (Si) in the form of powder and crystals has well-established procedures in the industry. Nevertheless, certain innovative methodologies have been documented for the reduction of silica (SiO_2) to yield silicon (Si). One such approach is electrochemical reduction, where silica is reduced to silicon through an electrochemical process. This method offers advantages such as lower process temperatures (less than 1000 °C) and the ability to carry out the reduction reaction at the contact point with an electrode [30]. This enables a more controlled and efficient reduction of silica to silicon.

Another method, carbothermal reduction, employs concentrated solar energy or biomass-derived carbon sources to undergo reduction of silica. This approach leverages the chemical reaction (Eq. (4)):

$$SiO_2 + C \rightarrow Si + CO_2 \tag{4}$$

Utilizing concentrated solar energy has the potential to serve as a practical heat source for driving the carbothermal reduction process. This approach involves concentrating the thermal energy from the sun, which is then harnessed to generate the elevated temperatures required for the decomposition of specific metal oxides [31]. Additionally, silica from rice husks, a waste product, can be utilized for the carbothermal reduction of silicon. For large-scale industrial production, carbothermal reduction in electric arc furnaces (EAFs) has long been the dominant and most economical method for extracting pure silicon from silica. This well-established process has benefited from continuous research and optimization over many years. However, recent advancements are pushing the boundaries with innovative approaches like the ultrafast carbothermal reduction using a CO_2 laser beam, pioneered by Maeng et al. [28]. The study demonstrated that the carbothermal reduction process could occur within seconds when the laser beam illuminated the silica/carbon mixture. While the research by Maeng et al. [28] demonstrated the significant influence of laser beam intensity and N_2 gas flow on the ultrafast carbothermal reduction process, it's important to consider its comparison to traditional methods. Conventional carbothermal reduction typically relies on large-scale facilities to effectively capture and utilize the high temperatures inherent to the process, maximizing thermal efficiency. This large-scale approach also often necessitates a stabilization step after initiating the reduction process to ensure consistent operation. In contrast, the laser-driven approach offers precise control over the localized area of reduction due to the focused nature of the laser beam. This potentially opens avenues for smaller-scale reactors and potentially avoids the need for a separate stabilization step. However, further investigation is needed to determine if the energy efficiency of the laser approach can match or surpass the well-established traditional methods. Through a comparison and contrast of the laser-driven approach with traditional carbothermal reduction, a deeper understanding of the trade-offs and potential benefits of this innovative technology is achieved. Approaches to silica reduction are

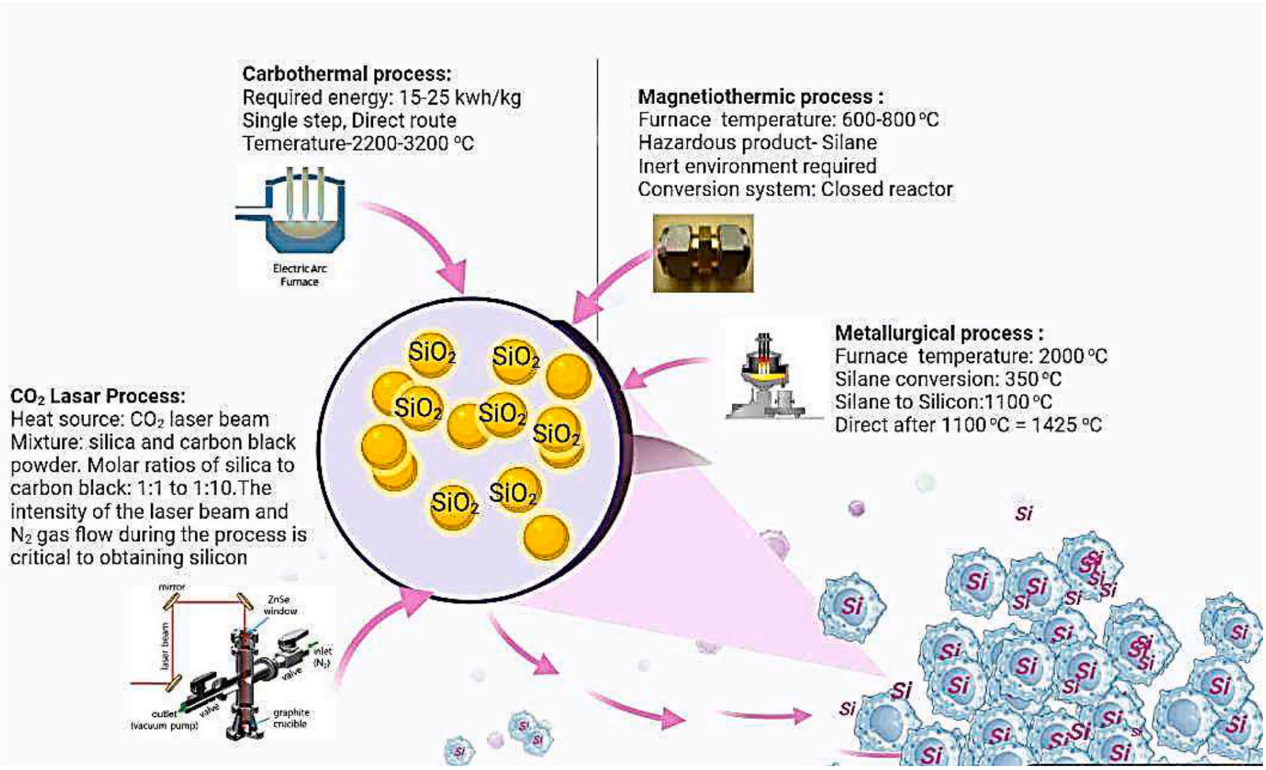

Fig. 3. Different routes to produce silicon from silica.

actively being explored by researchers, unlocking the potential for cleaner and more efficient silicon synthesis methods.

The carbothermal reduction process offers several advantages over the silicothermic process to produce silicon. By using carbon to reduce magnesium oxide, a process known as carbothermal reduction produces magnesium metal vapor and carbon monoxide gas at temperatures higher than 1600 °C [32]. While the established large-scale carbothermal reduction in arc furnaces proves efficient for metallurgical silicon production, it might not be the optimal choice for localized or small-scale extraction of silicon from silica. In such scenarios, a more scalable and adaptable approach for synthesizing silicon nanostructures (SiNSs) emerges in the form of combining ball milling of commercially available sands with magnesium reduction. However, when there is an excess magnesium-to-silica ratio in the reduction process, it often leads to the formation of magnesium silicide (Mg_2Si) instead of the desired silicon product for the final chemical reduction [33]. The final chemical reaction in this process involves the reduction of silicon dioxide (SiO_2) with magnesium to form silicon (Eqs. (4–6)).

$$SiO_{2(s)} + 2\,Mg_{(s)} \rightarrow 2MgO_{(s)} + Si_{(s)} \tag{4}$$

$$2\,Mg_{(s)} + Si_{(s)} \rightarrow Mg_2Si_{(s)} \tag{5}$$

$$Mg_2Si_{(s)} + 4HCl_{(aq)} \rightarrow 2MgCl_{2(aq)} + SiH_{4(g)} \tag{6}$$

The process involves the reduction of silica to magnesium oxide, the formation of magnesium silicide, and finally, the chemical reduction of magnesium silicide to produce silicon. This process allows for the synthesis of silicon with controlled nanostructures and has potential applications in photocatalytic applications. During the etching process of silicon with hydrochloric acid (HCl), some of the magnesium silicide produced can react with the acid, resulting in the formation of silane gas (SiH_4) and other hazardous byproducts. Silane is a pyrophoric gas, meaning it can ignite spontaneously upon contact with air. When silane reacts with air, it can cause tiny explosions on the surface of the acid, even without any external ignition source [34]. This poses a significant safety risk, and fatal industrial accidents resulting from the combustion and detonation of leaked silane in the air have been reported. To ensure safety, the silane gases discharged during the reaction with HCl are diluted with an inert gas, such as nitrogen (N_2). Diluting the silane gas helps to inhibit its further reaction with oxygen in the air, preventing the formation of silicon dioxide. This suppression of the reaction between the hazardous byproducts and oxygen is crucial in preventing the formation of silicon dioxide during the etching process. On the other hand, when silicon dioxide (SiO_2) reacts with hydrofluoric acid (HF), it forms silanol bonds on the silicon dioxide surface. The fluorine species in the HF solution then react with the silicon, resulting in the formation of silicon tetrafluoride gas (SiF_4), which is soluble in water and forms hexafluorosilicic acid (H_2SiF_6) (Eq. (7)).

$$SiO_{2\ (s)} + 6HF_{(aq)} \rightarrow H_2SiF_{6(aq)} + H_2O \tag{7}$$

This reaction helps in the removal of silicon dioxide during etching, facilitating the desired process [35]. It is important to handle these reactions with appropriate safety measures to ensure the well-being of personnel and prevent any potential hazards.

The electrical properties of metallurgical silicon, despite being a commonly used material, deteriorate due to flaws and recombination centers introduced by the material's impurity [36]. These defects and recombination centers also cause a shortening of the carrier lifetime and a decrease in conductivity. This makes metallurgical silicon less suitable for electronic applications, and purification and refinement processes are typically required to improve its electrical properties for further utilization. Size reduction has shown promise in enhancing the electronic activity of metallurgical silicon. The transition from anisotropic to isotropic etching of the nanoparticles, along with the effects of surface properties and surface-to-volume ratio, contribute to the enhanced reactivity of smaller particles [37]. Furthermore, particle size reduction has been shown to have a positive impact on the photocatalytic performance of metallurgical silicon. Lv et al. [38] reported a significantly increased H_2 evolution rate in photocatalytic reactions when using smaller metallurgical silicon particles. However, it should be noted that severe degradation issues may arise simultaneously. A significant challenge associated with silicon, including metallurgical silicon, is its high optical reflectance (~40 % in specific wavelength ranges). This poses limitations in applications where high light absorption is crucial, such as photocatalysis. To overcome this limitation, surface etching techniques are employed to enhance the light absorption capabilities of silicon, particularly within the desired optical spectrum.

The formation and growth of silicon nanoclusters (SiNCs) and their transformation into nanocrystals or crystalline silicon are indeed temperature-dependent processes. Different silicon-rich precursors and experimental conditions can lead to variations in the specific temperature ranges and conditions involved in these processes. One example is the conversion of silicon monoxide (SiO) during pyrolysis. The pyrolysis of hydrogen silsesquioxane (HSQ) in the thermal disproportionation method is believed to undergo dehydrogenation, crosslinking, and decomposition stages [39], as shown in Fig. 4. These three stages collectively describe the pyrolysis process of HSQ in the thermal disproportionation method. By understanding and controlling these stages, researchers can optimize the synthesis conditions and obtain desired silicon-based materials with specific properties. Below 300 °C, the silicon phase exists as a single, randomly bonded structure resembling SiO, often denoted as "SiO-like." As the temperature escalates from 400 °C to 800 °C, a remarkable transformation unfolds. Amorphous

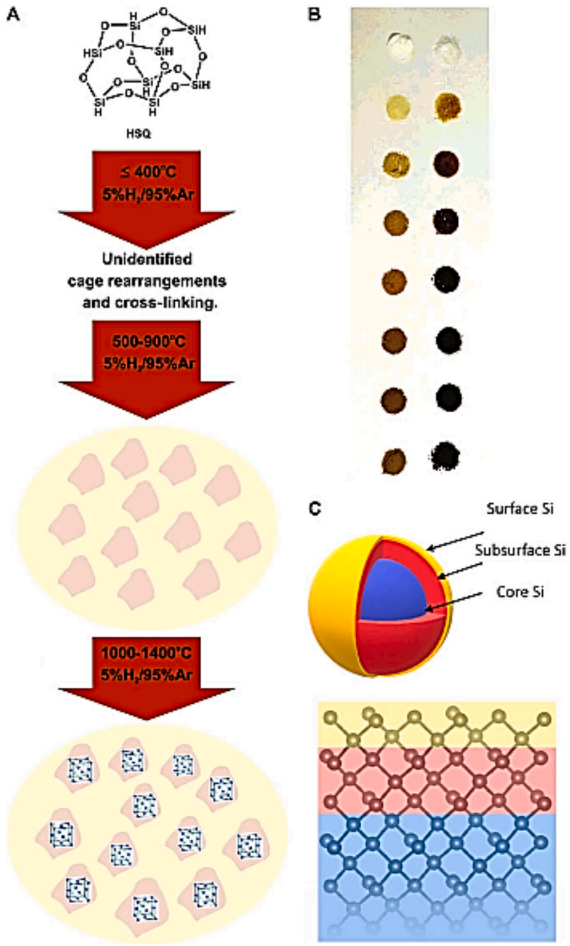

Fig. 4. Three stages of the thermal disproportionation process from room temperature to 1400 °C for HSQ.

(non-crystalline) nanoclusters rich in silicon begin to nucleate and progressively enlarge. This growth is attributed to the release of excess silicon atoms within the material, facilitating the aggregation and coalescence of these clusters. Finally, upon reaching a critical temperature window between 800 °C and 900 °C, a dramatic shift occurs: the amorphous silicon undergoes crystallization [40]. This phase transition signifies the emergence of well-defined, ordered crystalline silicon structures. For silicon-rich oxide films, researchers have proposed a two-stage thermal disproportionation process to explain their behavior at elevated temperatures. Once the temperature surpasses 500 °C, the first stage commences. During this stage, precipitation of silicon from the oxide matrix takes place. This initial precipitation event sets the stage for the subsequent development and evolution of the distinct silicon phase. In the second stage, at even higher temperatures, typically above 1000 °C, the excess silicon crystallizes [41]. These studies suggest that amorphous materials require reaching a threshold temperature to initiate crystallization. The growth of nanoclusters in this temperature range primarily depends on temperature rather than the composition of the material. The diffusion coefficient, which affects the growth kinetics, is not significantly influenced by the composition. It is important to note that the specific temperature ranges and conditions may vary depending on the precursor, experimental setup, and other factors [42]. Understanding the temperature-dependent processes involved in the formation and transformation of silicon nanoclusters is crucial for controlling their properties and tailoring them for various applications.

High surface area mesoporous crystalline silicon can be produced via the bottom-up self-templating synthesis process based on $SiCl_4$ reduction. To construct the mesoporous structure, this technique uses salt by-products as pore templates. This self-templating technique was used by Dai et al. [43] to successfully manufacture nanosized mesoporous crystalline silicon powders. Mesoporous crystalline silicon (Si) powders have been investigated for their exceptional activity in the HER, as demonstrated by Dai et al. [43]. This remarkable performance can be associated with the powders' unique structural characteristics, particularly their extensive surface area. This large surface area promotes an increase in the availability of reaction sites and facilitates mass transport, ultimately leading to the observed enhanced HER activity. Numerous techniques have been investigated for the fabrication of 2D Si nanosheets (SiNSs). By using a Grignard reagent and polysilane as catalysts in a chemical reaction, Okamoto et al. successfully produced organosilicon nanosheets. The fabrication of SiNS structures with constrained dimensions is possible using this technique [44].

Several advantages are presented by 2D Si nanosheets as photocatalysts for the hydrogen evolution reaction (HER). Interaction with reactant molecules is facilitated, and reaction kinetics are enhanced. Efficient adsorption and participation of water molecules in the HER process are enabled by the exposed surface. This allows for the tailoring of electronic and catalytic properties to optimize HER performance. However, a significant challenge is posed by the widespread production of highly pure Si nanosheets. Processes that involve gas-phase growth have purity or size distribution restrictions, as do methods that use metal doping or methylamines. For instance, Joo et al. [45] successfully achieved the catalyst-free synthesis of freestanding silicon nanosheets (SiNSs) through the chemical vapor deposition (CVD) of $SiCl_4$ under high-flux H_2 reaction conditions. Despite producing SiNSs, this method is less suited for manufacturing at a low cost due to its wide size distribution and production constraints in large quantities [45]. This research emphasized to development of scalable and effective processes for producing high-quality SiNSs and mesoporous crystalline silicon materials for a variety of uses, including photocatalysis. The size of SiNCs cannot be precisely controlled with electrochemical etching or laser ablation, despite their simplicity and effectiveness. The etching process of a silicon wafer involves selectively removing or modifying the surface layer of the silicon material using chemical or physical methods. Etching is commonly performed in the fabrication of various photocatalysts. There are different etching techniques used in silicon wafer processing are shown in Fig. 5A.

A groundbreaking investigative effort by Yang et al. [46] has introduced a novel methodology for silicon surface etching. This innovative approach leverages the synergistic combination of two powerful tools: laser-induced terahertz emission spectroscopy (TES). By integrating these techniques, the researchers unlock valuable insights into the etching process, enabling precise control and optimization. By using BHF etching, they removed the native oxide layer, creating a partial negative charge on the fluorine-terminated surface. Further etching transformed it into a fully hydrogen-terminated state (Fig. 5B). They observed changes in THz emission and surface conditions based on different Si doping types and concentrations The intriguing polarity-dependent response of silicon (Si) surfaces to terahertz (THz) radiation, along with associated variations with doping and etching, is manifested. Specifically: In the case of n-type Si, a decrease in THz emission is observed upon the reversal of applied polarity, indicating a heightened interaction between the THz field and surface charges in this configuration. For both $n + -$type Si and undoped Si, in contrast, an increase in THz emission is observed after polarity reversal. This phenomenon may be attributed to alterations in surface carrier dynamics or changes in the optical properties of the near-surface region. In p-type Si, initial polarity reversal results in an increase in THz emission, followed by a subsequent decrease. This pattern indicates a complex interplay between surface properties and the THz field. Moreover, the modulation of THz emission polarity and the influence on the removal of the native oxide layer during etching, as depicted in Fig. 5C, are significantly affected by the etching time.

The specific nature of this dependence is presumed to arise from changes in surface morphology, defect states, and carrier lifetimes due to the etching process. These observations underscore the intricate interplay among the electrical properties, doping, and surface characteristics of Si, collectively influencing its interaction with THz radiation. Further investigation into the underlying mechanisms driving these polarity-dependent responses and the impact of etching protocols holds promise for tailoring the THz emission properties of Si surfaces, potentially advancing applications in sensing, imaging, and communication technologies. The THz emission polarity and the removal of the native oxide layer were also influenced by the etching time (Fig. 5C). This process leads to the formation of a hydrogen (H)-terminated surface. Interestingly, this transformation is accompanied by a polarity reversal in the terahertz (THz) emission amplitude, shifting from positive to negative. When a protective layer (PR) is present, the amplitude polarity in protected areas stays positive. However, upon removing the PR, the amplitude in the unetched area experiences a slight decrease. A notable decrease in measurement values has been observed, potentially attributable to the lingering presence of water on the surface. This surface water is hypothesized to introduce a systematic error into the measurement process, thereby leading to the observed underestimation of true values. Further investigation into the mechanisms by which residual water influences measurements and the implementation of suitable mitigation strategies are crucial for ensuring accurate and reliable data acquisition.

Each technique has its advantages and is selected based on the specific requirements of the fabrication process. It's important to note that the etching process can be controlled by factors such as etchant composition, temperature, time, and mask patterns used to protect certain areas of the wafer. These factors determine the etch rate, selectivity, and profile of the etched features. The use of laser ablation is constrained by the need for complex equipment. Plasma synthesis is a desirable alternative despite requiring specialist equipment since it delivers high yield and surface hydride termination. The high productivity and practicality of solution-phase synthesis make it advantageous. The probable inclusion of carbon impurities in the product has aroused some concerns, though, and this needs to be taken care of. The synthesis of SiNC can be accomplished using thermal disproportionation or pyrolysis of silicon-rich oxides. The thermal disproportionation of silicon-rich

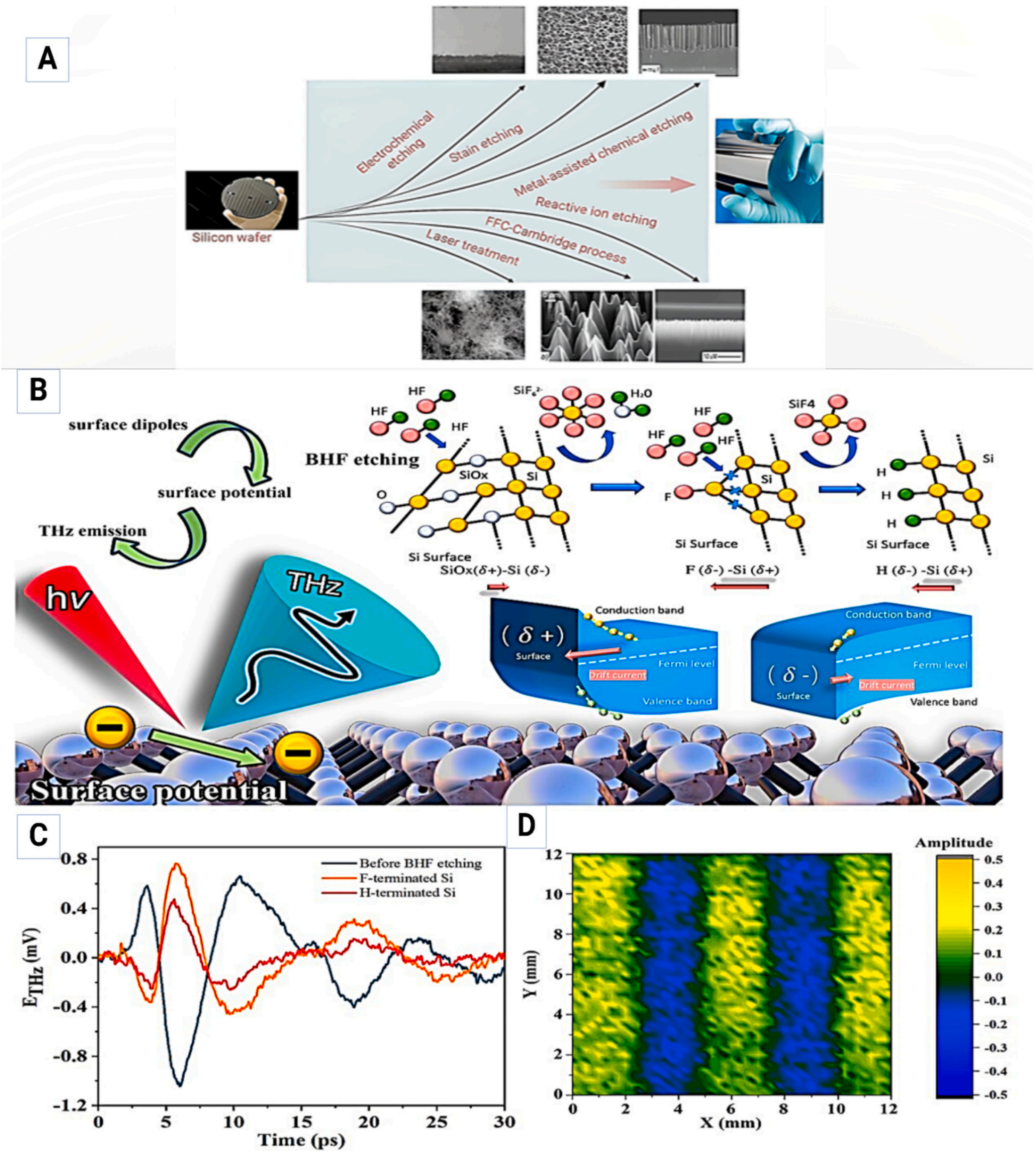

Fig. 5. A. The different etching processes of a silicon wafer; B. The terahertz (THz) emission mechanism from a silicon (Si) surface with laser excitation and the chemical process involved in BHF (Buffered Hydrofluoric Acid) etching. C. The THz emission waveforms on a low-doped n-type Si surface can be different before BHF etching, in the F-terminated condition, and the H-terminated condition. D. LTEM (Low-energy Transmission Electron Microscopy) images of a silicon (Si) sample can be obtained after applying a 2.5 mm interval line-space structure of photoresist on the surface and subsequent BHF etching. The Si sample is subjected to a 1 % dilute BHF etching process for 300 s. Afterward, the photoresist is removed from the surface.

oxides combines size tunability, excellent production yields free of carbon contamination, and clear processing techniques. The SiNCs produced by this approach can be surface functionalized, and it has been widely used to explore the chemical and physical characteristics of SiNCs.

The development of silicon (Si)-based photocatalysts has been actively pursued owing to their In recent advancements, various synthesis approaches have been utilized to modify Si morphology, doping levels, and surface chemistry to optimize photocatalytic performance. It has been observed that the photocatalytic efficiency of Si is significantly influenced by its structural attributes such as shape, size, and crystalline phases. These factors determine the availability of active sites and the behavior of charge carriers. Among the different fabrication routes, the electrochemical and carbothermal reduction of silica have been extensively investigated. In particular, the laser-driven carbothermal reduction process has shown potential for localized and ultrafast silicon synthesis, although further studies are warranted to assess its scalability and energy efficiency compared to conventional electric arc furnace-based methods. Magnesium reduction methods, while effective in generating silicon nanostructures, have been associated with hazardous byproducts such as silane (SiH_4), necessitating stringent safety protocols. The etching processes, both chemical and physical, have also been explored to tailor surface properties and reduce reflectivity, thereby enhancing light absorption—a critical parameter for photocatalysis. Thermal disproportionation methods, especially those involving silicon-rich oxides such as hydrogen silsesquioxane (HSQ), have been employed to obtain nanocrystalline silicon with controlled size and minimal impurities. These bottom-up techniques are preferred for their tunability and ability to avoid carbon contamination. While promising methods such as plasma and solution-phase synthesis offer high yields and tunability, concerns regarding contamination and complexity persist. It is suggested that future research should focus on scalable, environmentally benign, and controllable synthesis pathways to fabricate high-performance Si photocatalysts suitable for diverse energy and environmental applications.

4. Advances in nanostructured photocatalysts for hydrogen production

Nanostructured photocatalysts have shown significant promise for hydrogen production through photocatalytic water splitting. These materials offer several advantages, including increased surface area, improved light absorption, enhanced charge separation, and reduced recombination rates, leading to enhanced photocatalytic activity. These recent advances in nanostructured photocatalysts provide opportunities for the development of efficient and sustainable hydrogen production systems. These efforts concentrate on meticulously refining the design, synthesis, and integration of photocatalytic materials, with the ultimate goal of maximizing solar-to-hydrogen generation efficiencies and paving the way for widespread implementation. The introduction of lattice defects or dopants in small quantities can significantly modify the material properties of Si photocatalysts. Even a tiny amount of dopant can induce changes such as increased conductivity in insulating materials or the formation of recombination centers in perfect crystal structures. These alterations can enhance carrier transport properties and improve the efficiency of charge separation and utilization. A recent advance in nanostructured photocatalysts for hydrogen production has been discussed in the subsequent sections.

4.1. Black silicon composite

Black silicon (bSi) has arisen as a prospective material for solar cells owing to its enhanced capacity to efficiently absorb and harness infrared light in comparison to conventional silicon solar cells. The process of creating black silicon involves striking solar cells with lasers in the presence of sulfur gas, which changes the texture of the cells' surface and incorporates sulfur atoms into the silicon lattice [47]. This modification gives the material its black appearance. One of the main advantages of black silicon is its enhanced photon absorption and light-trapping capabilities.

Black silicon has been reported to have high absorption capabilities for photons, typically around 99 % [48]. Different studies may report slightly different absorption percentages based on their experimental setups and methodologies. The unique surface structure of black silicon, which consists of randomly arranged silicon nanowires or nanopillars, allows for enhanced light trapping and absorption. For solar cells to convert sunlight into electricity with maximal efficiency, enhanced light absorption within their active materials is paramount. This phenomenon plays a pivotal role in maximizing the number of photons captured and subsequently converted into charge carriers, contributing directly to the overall power output of the device. By maximizing the number of photons captured and subsequently converted into electrical energy, this improvement translates to a heightened overall power output of the device. By achieving a high absorption rate, black silicon can potentially capture a larger portion of the solar spectrum, including a broader range of wavelengths. This expanded absorption range can be advantageous for solar energy conversion, especially in situations where traditional silicon solar cells may have limitations. It's worth noting that the actual absorption efficiencies of black silicon can vary depending on the specific fabrication techniques, surface textures, and other factors [49].

The surface of black silicon contains pillars with varying sizes and spacings, creating a well-like structure. The fostering of multiple interactions between incoming photons and the material is facilitated by the unique micro- and nano-structured surface morphology of black silicon, thereby enhancing the probability of photon trapping and absorption [50]. Two distinct mechanisms are effectively employed by this intricate architecture: For Lightwave Guiding, the enhanced penetration of higher-energy photons deeper into the material is facilitated by the strategically designed wells within the black silicon structure, which function as waveguides. This extended path length increases the likelihood of these photons interacting with and being absorbed by the silicon lattice. For the case of scattering and trapping, alterations in direction and potentially energy of photons occur as they traverse and scatter within the maze-like network of wells. Notably, these scattering events selectively diminish the energy of departing photons, reducing the likelihood of their escape back into the environment and contributing to their confinement and subsequent absorption within the black silicon structure. By synergistically combining these guiding and scattering phenomena, the efficient harvesting and utilization of light energy is passively facilitated by the unique surface features of black silicon, thereby advancing the performance of photovoltaic devices and other light-sensitive applications.

As a result, black silicon can effectively capture a broader range of wavelengths and increase the overall optical absorption of the material [50]. The refractive index of black silicon exhibits variation along the height gradient of the pillars. This refractive index heterogeneity induces multiple scattering of wavelengths possessing distinct wave phases, thereby augmenting the likelihood of absorption by the black silicon material. The combination of well-like structures and refractive index variations makes black silicon an efficient absorber of photons, contributing to its improved light-trapping capabilities. By replacing traditional silicon with black silicon, the optical absorption of the material is significantly increased, reducing the amount of light reflection (which can be as high as 40 % in silicon) and maximizing light collection. This enhancement in light absorption improves the photocatalytic behavior of semiconductors like TiO_2, leading to improved overall performance in photocatalytic processes. Researchers have also explored the use of black silicon composites, such as combining black silicon substrates with gold (Au) particles. These composites have exhibited diminished optical reflection across a wide wavelength spectrum, thereby amplifying light collection capabilities and enhancing the photocatalytic performance of semiconductor materials, such as TiO_2.

Garin et al. [51] focused on black silicon-induced junction photodiodes and investigated their performance in terms of external quantum efficiency (EQE) and spectral response. They observed external quantum efficiencies of conelike morphology above 130 % in black silicon-induced junction photodiodes (Fig. 6A-6B). The enhanced EQE was particularly evident at a wavelength of 200 nm, where the EQE values reached up to 132 %. This suggests that black silicon can effectively convert incident photons into charge carriers in the ultraviolet range. Black silicon was found to enable broader responsiveness to a wider range of light wavelengths (Fig. 6C). This characteristic expands the potential applications of black silicon photodiodes to different parts of the electromagnetic spectrum. The study conducted by Garin et al. [51] suggested that due to the unique surface structure of black silicon, it can create additional charge carriers through a process called impact ionization. Impact ionization occurs when high-energy photons generate electron-hole pairs, and these pairs generate more carriers than the number of photons absorbed (Fig. 6D). This phenomenon can potentially lead to an effective efficiency exceeding 100 %. It's important to note that the concept of efficiency exceeding 100 % is based on the idea that impact ionization can generate additional carriers beyond the number of photons absorbed. However, it's crucial to approach such claims with caution and await further research and verification from the

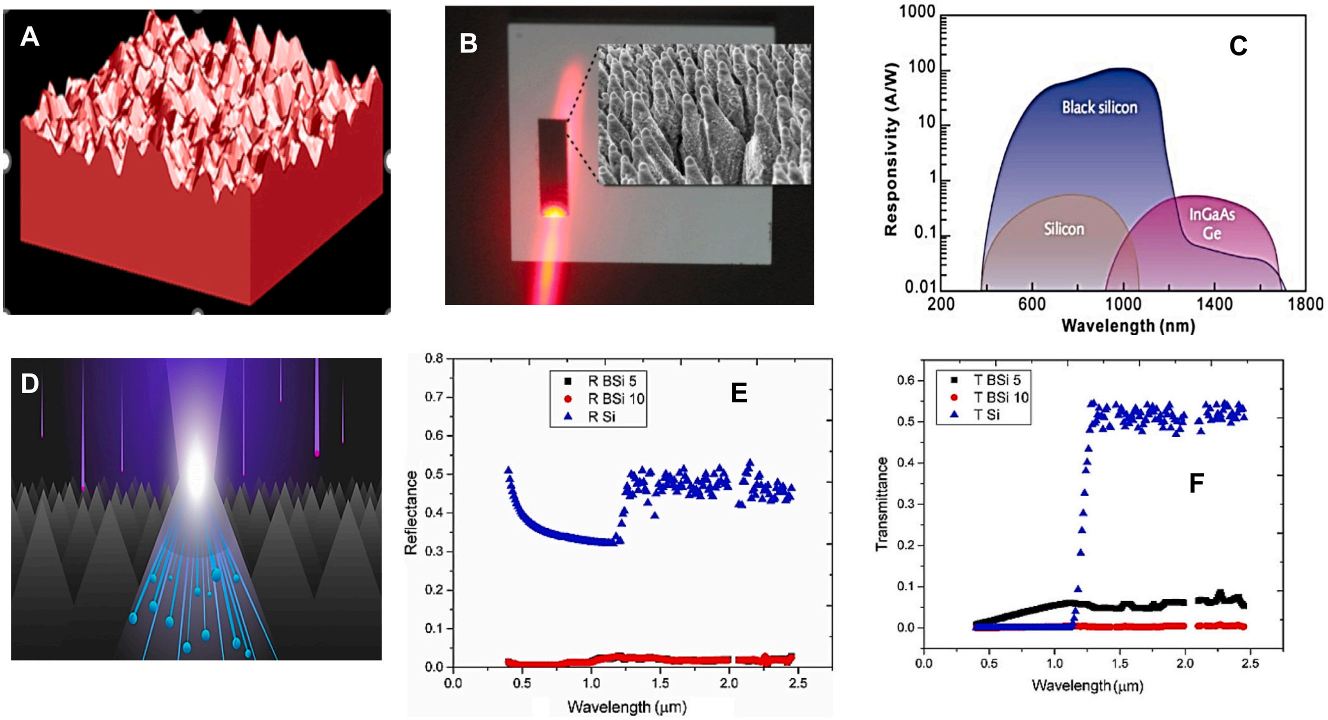

Fig. 6. A. 3D view of Black silicon. B. SEM image of black-Si nanotexture with conelike morphology; C. Black silicon enables broader responsiveness to a wider range of light wavelengths, D. Generation additional charge carriers through an impact ionization process. E. Comparison plot of simulated reflectance of pristine Si and B—Si. F. Generation of additional charge carriers through an impact ionization process. E. Comparison plot of simulated transmittance of pristine Si and B—Si.

scientific community.

Black silicon is characterized by its roughened surface with randomly oriented nanoscale spikes or structures, which result in reduced transmittance and reflectance of light [52]. Marthi et al. [53] used an effective medium approximation model to determine the optical constants of black silicon. They found that black silicon exhibits significantly lower reflectance compared to pristine silicon, while its transmittance is consistently low across different thicknesses (Fig. 6E and Fig. 6F). These optical properties indicate that black silicon absorbs a larger fraction of incident light, making it advantageous for photocatalysis and hydrogen production. The low transmittance allows for efficient utilization of a broader range of the solar spectrum, leading to improved light absorption and enhanced photocatalytic activity. Additionally, the low reflectance ensures that a higher percentage of incident light is absorbed by black silicon, facilitating the generation of photoexcited electrons necessary for the hydrogen evolution reaction. The combination of low transmittance and low reflectance in black silicon maximizes light absorption and utilization, resulting in higher photocatalytic activity and increased overall efficiency in converting solar energy into hydrogen.

The exceptional light management exhibited by black silicon arises from the intricate synergy of its multiscale surface texture, as elucidated by Ao et al. [54]. The intriguing textural landscape described features both nano-sized blade-like structures and micro-sized modulated pores, intricately intertwined to achieve efficient light trapping and absorption across a broad spectrum. This synergistic combination of features warrants a closer scientific examination to unravel the underlying mechanisms contributing to its remarkable performance. Specifically, the textured surface facilitates the coupling of short-wavelength light, enabling its effective capture and utilization within the material. In addition, the modulated pores function as efficient scattering centers for long-wavelength light, redirecting photons and increasing their path length within the silicon, ultimately enhancing their probability of absorption. The practical significance of enhanced light harvesting in photocatalytic water splitting is convincingly exemplified by the work of Ao et al. [54]. They observed a remarkable 45 % increase in photocurrent density achieved through the use of black pn-silicon coated with TiO_2 compared to a control sample. This observation merits a closer scientific examination to illuminate the underlying mechanisms responsible for such an impressive improvement. This significant improvement can be directly attributed to the superior light absorption capabilities of black silicon, highlighting its potential to boost the efficiency of light-driven processes.

The exploration of the potential of controllably grown $(Ga_{1-x}Zn_x)(N_{1-x}O_x)$ nanorods on black silicon as anodes for water splitting has been undertaken [55]. To realize this, the direct growth of $(Ga_{1-x}Zn_x)(N_{1-x}O_x)$ nanorods onto black silicon as anodes for water splitting was pursued, as illustrated in Fig. 7A. The in-situ growth of black silicon and the $(Ga_{1-x}Zn_x)(N_{1-x}O_x)$ solid solution ensured a robust adhesion between the two materials. The resultant black silicon/$(Ga_{1-x}Zn_x)(N_{1-x}O_x)$ samples, when utilized as photoanodes in photoelectrochemical (PEC) water splitting, manifested superior performance compared to photoanodes based on single-crystal silicon (SC-Si)/$(Ga_{1-x}Zn_x)(N_{1-x}O_x)$. The incorporation of black silicon in the photocatalyst structure improved the efficiency of the photoelectrochemical water-splitting process. These studies highlighted the potential of black silicon in enhancing light absorption and improving the performance of photocatalytic and photoelectrochemical processes. The unique surface texture of black silicon enables efficient light utilization and offers advantages in various applications, including water splitting for renewable energy production. The development and optimization of black silicon-based materials continue to be an active area of research to further enhance their performance.

By decoupling the carrier generation in different junctions, researchers can tailor the design parameters of each junction independently to maximize their performance. This approach provides greater freedom in optimizing the materials, bandgaps, and other parameters of

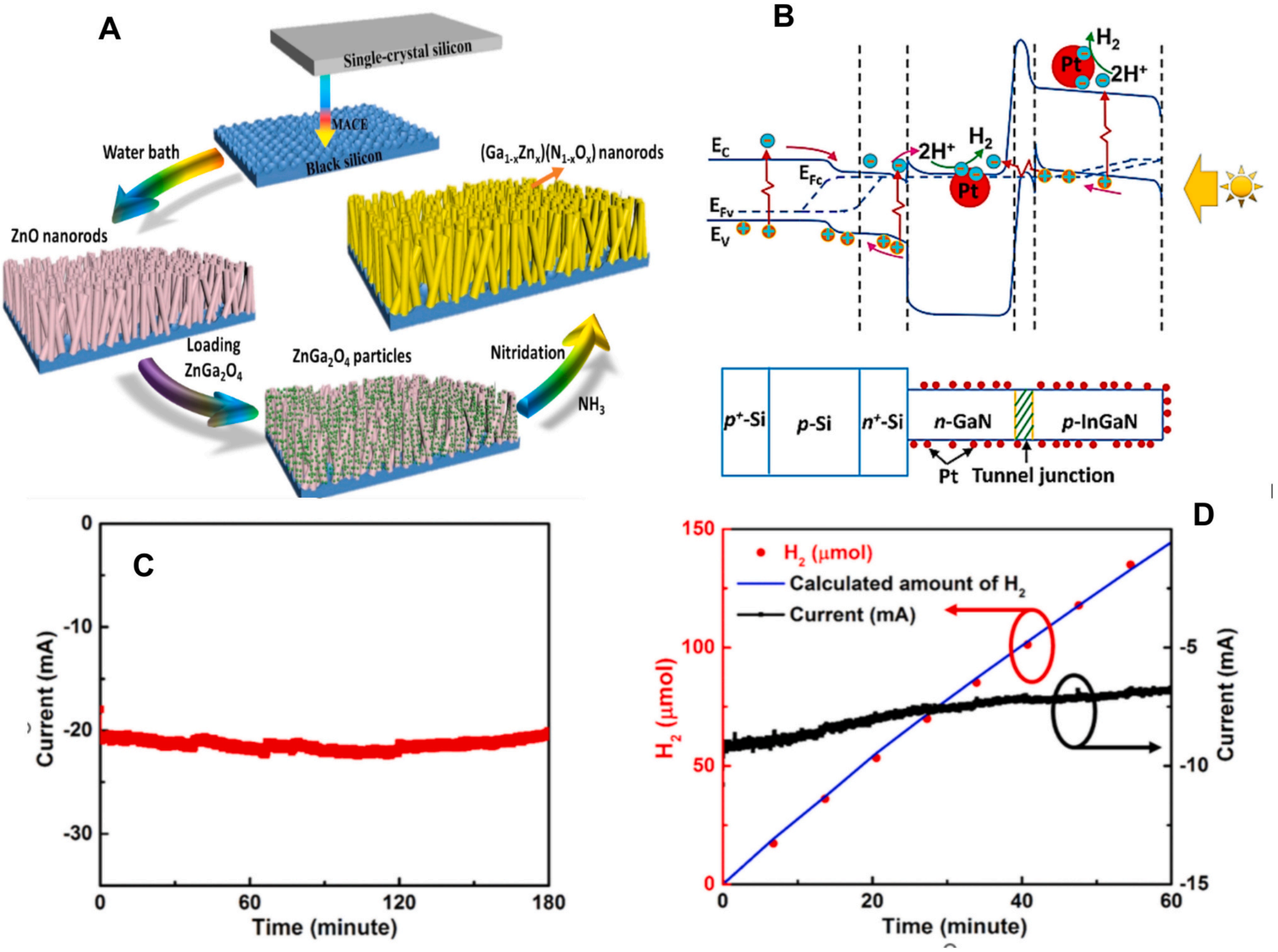

Fig. 7. **A.** The synthesis of nanorods; **B.** The energy band diagram of InGaN tunnel junction nanowires on an n + −p Si substrate under illumination. **C.** Under 1.3 sun of AM1.5G illumination, a stable photocurrent was observed for a duration of 3 h at an applied bias of 0.06 V versus the normal hydrogen electrode (NHE). This indicates that the system maintained a consistent current output over time, demonstrating its stability [56]. **D.** The hydrogen generation efficiency was assessed by measuring the amount of H_2 produced at different times under 1.3 sun of AM1.5G illumination and an applied voltage of 0.26 V versus NHE. The red dots in the experimental data represent the measured amount of H_2 generated at various time points. The black curve represents the photocurrent, which serves as an indicator of the electron flow during the photocatalytic process. The blue curve represents the theoretical amount of H_2 expected based on the photocurrent, assuming a 100 % Faradaic efficiency. Faradaic efficiency refers to the extent to which the consumed electrons are used for the desired reaction, in this case, the production of H_2 [56]. (For interpretation of the references to colour in this figure legend, the reader is referred to the web version of this article.)

individual junctions, which can lead to improved overall device efficiency. By overcoming the hurdle of equal carrier generation, Fan et al. [56] lateral extraction scheme opens doors to designing and optimizing multijunction photoelectrodes for maximum efficiency. This innovative approach paves the way for significant advancements in multijunction photoelectrode performance by offering greater design freedom for carrier extraction. The vertical arrangement of the heterostructure, as depicted in Fig. 7B through its energy band diagram, underscores the tiny difference in energy levels where electrons can move between silicon and gallium nitride. The small conduction band offset and heavy n-doping allow excited electrons from the silicon to seamlessly flow into the nanowires, where they either power hydrogen production directly or recombine with partner holes. For even better performance and longevity, consider layering a protective shield on the device. This shield would blanket the exposed silicon surface and the critical junction with indium gallium nitride, optimizing the efficiency of the underlying solar cell wafers by minimizing degradation and maximizing light absorption. Fan et al. [56] delved into the stability and degradation mechanisms of the InGaN/Si photocathode, with a particular focus on the impact of the onset potential shift and surface preparation conditions, as illustrated in Fig. 7C and D. Rapid InGaN/Si photocathode degradation linked to onset potential shift, possibly due to GaN/Si interface SiNx layer etching. Interface degradation via SiNx layer etching at the GaN/Si heterojunction manifests as increased interfacial resistance and a positive shift in onset potential. Notably, preparing the silicon substrate surface influences the formation and properties of the amorphous SiNx layer, leading to variations in device stability, as evidenced by the observed differences. The work of Fan et al. [56] introduces a promising and flexible design approach for multijunction photoelectrodes, exemplified by the InGaN/Si tandem system. Further optimization through protective layer implementation and a deeper understanding of degradation mechanisms hold immense potential for enhancing the efficiency and stability of these devices.

The study by Kan et al. [57] focused on the development of a highly active photocatalyst for photoelectrochemical (PEC) applications. The researchers aimed to improve both the electrochemical activity and stability of the photocatalyst. The photocatalyst system they investigated consisted of a titanium dioxide (TiO_2) layer, an iridium oxide (IrOx) layer, and a porous silicon (por—Si) skeleton. The first layer (TiO_2) captured light, and the second layer (IrO_x) helped the light-driven reaction happen faster. However, the porous silicon skeleton, although advantageous for its large surface area and adherence to supported catalysts, was prone to photo-corrosion. To mitigate the photo-corrosion issue, Hossen and Ismail, [58] deposited a thin layer of α-Fe_2O_3 (alpha-Fe_2O_3) on the surface of the porous silicon to form a p-n junction. This junction helped minimize the photo-corrosion of the porous silicon skeleton, thereby increasing the stability of the photocatalyst. Several inherent properties of black silicon endow it with high advantages as a conductive substrate in photoelectrochemical (PEC) applications. Black silicon's intricate structure of pores acts like a light trap, gobbling up incoming photons and boosting the amount of visible light absorbed within the material. This translates directly into a substantial improvement in the overall efficiency of the photocatalytic process. The increased specific surface area of black silicon, in comparison to flat silicon substrates, equates to a greater number of reaction sites available for the photocatalytic reaction. This abundance of reaction sites directly contributes to higher catalytic activity, thereby augmenting the performance of the system. The increased roughness associated with the porous structure of black silicon facilitates improved adherence for supported photocatalysts. The precise design of photocatalyst systems often prioritizes the optimization of interfacial contact between the substrate and the catalyst. This strategic approach fosters enhanced separation of photogenerated electrons and holes, ultimately culminating in an amplified overall performance of the system. A closer scientific examination reveals the underlying mechanisms driving this synergistic effect. The unique combination of light trapping, high surface area, and improved catalyst adherence offered by black silicon establishes it as a valuable material for advancing the efficiency and performance of PEC applications.

Light absorption is significantly improved in bSi through the formation of nanoscale surface features such as conical spikes, nanowires, or pores, which are typically created via laser irradiation in a sulfur-rich atmosphere. These structures have been reported to reduce reflectance and enhance light trapping by facilitating multiple scattering and guiding phenomena within the material. Consequently, photons are more likely to be absorbed and converted into charge carriers, thereby improving device performance. This enhanced light absorption, often approaching 99 %, has been achieved by leveraging the gradient refractive index along the height of the nanostructures, which increases the optical path length of incoming photons. Particularly noteworthy is the role of bSi in broadening the absorption spectrum to include infrared and ultraviolet regions, allowing for improved spectral utilization. The surface morphology has also been demonstrated to increase the probability of impact ionization, potentially leading to external quantum efficiencies exceeding 100 %, a phenomenon that warrants further investigation and validation. While the advantages of black silicon are compelling, it must be emphasized that issues related to surface stability and degradation especially at heterojunction interfaces—must be rigorously addressed.

4.2. Silicon nanosheets composite

The properties of 2D nanosheets make them highly advantageous for various applications, including fast interfacial charge transfer and efficient photocatalysis. The properties of nanosheets can be modified by adjusting their thickness, incorporating heteroatoms, or subjecting them to external stimuli such as electric fields, strain, or illumination. This tunability allows for the engineering of 2D materials specifically for hydrogen (H_2) production, among other applications. By reducing the dimensions of semiconductors to ultrathin structures, the generated charge carriers inside the material can efficiently migrate to the surface, facilitating their participation in photoreactions. This rapid movement of charge carriers reduces the chances of recombination within the semiconductors, which can hinder overall photocatalytic efficiency [59]. Furthermore, the ultrathin layered hollow structure of nanosheets enhances the reaction contact area, leading to an increased surface area available for catalytic reactions. This enlarged contact area provides numerous catalytic sites, which can significantly enhance the efficiency of the desired chemical reactions.

The specific types of nanosheet silicon composites reported in the literature (Fig. 8) can vary depending on several factors, including the preparation procedure, precursor materials, and other influencing factors. The structure and properties of nanosheet silicon composites are significantly influenced by the preparation procedure. It may involve techniques like sol-gel synthesis, chemical vapor deposition, electrodeposition, or other specific methods tailored to the desired composite structure. Additionally, precursor materials, such as silicon precursors, carbon sources, metal precursors, or polymers, can be selected based on the desired properties and compatibility with the nanosheet silicon synthesis process. It is worth emphasizing that the specific types of nanosheet silicon composites and their characteristics continue to evolve as researchers explore new synthesis methods and investigate various material combinations.

The combination of ball milling of commercial sands with magnesium reduction is a widely utilized technique in the manufacture of silicon nanosheets (SiNSs). This technique, however, frequently produces SiNSs that are fragmented into tiny bits and stacked together, which reduces their effectiveness in a variety of applications. Ryu et al. [61] suggested an alternative synthesis method to get high-purity SiNSs to solve this problem. They used a high-temperature molten salt, such as NaCl, which accomplished two tasks at once: it induced SiNS exfoliation and aided in the simultaneous chemical reduction of clays. With a rate of 486 mol H_2 per hour per gram of Si, they were able to successfully produce SiNSs that displayed excellent performance in photo-assisted hydrogen production. This improved performance was attributable to the SiNSs' huge specific surface area and distinctive shape. The researchers also found that the rate of hydrogen evolution dramatically enhanced to 723 mol H_2 per hour per gram of Si under visible light (with a wavelength of about 400 nm) by adding platinum nanoparticles (Pt NPs) as a cocatalyst to the SiNSs. Adding platinum nanoparticles (Pt NPs) as a co-catalyst significantly boosted its overall efficiency. Notably, this increased rate was maintained for at least 26 h without noticeably decreasing the catalyst activity, demonstrating the stability of the SiNSs and Pt NPs as a photocatalytic system.

The presence of ultrathin nanosheets with a hierarchically porous structure has been found to significantly enhance photocatalytic hydrogen (H_2) production compared to catalysts with a hexagonal nanorod structure. The randomly branched nanosheets offer a more active surface area, which leads to increased light-harvesting efficiency due to their shorter electron diffusion path. The hierarchically porous structure of the nanosheets further contributes to improved light absorption by creating a trapping light structure. This structure enhances the specific surface area of the catalyst and provides additional photocatalytic reaction sites. Consequently, the nanosheets exhibit enhanced efficiency in the photocatalytic reaction, particularly under visible light irradiation. Visible light excitation leads to the production of hydrogen and hydroxyl radicals on the metals present in the catalyst, highlighting the effectiveness of these ultrathin nanosheets in utilizing visible light for the photocatalytic process [68]. Additionally, the larger roughness of the nanosheets promotes good adhesion to supported catalysts. The stronger bond between the materials, acts like a superhighway for photogenerated electrons and holes, significantly accelerating their separation and boosting the photocatalytic reaction [68]. Efficient charge carrier separation helps prevent their recombination, allowing them to participate in surface reactions more effectively and contribute to the desired photocatalytic processes.

Siloxene, a two-dimensional silicon oxide material with a distinct low-buckled structure, has gained significant attention due to its unique properties. While siloxene offers a stable structure with low free energy, it can also exist in an amorphous phase due to the random arrangement of oxygen atoms. A recent study by Zhou et al. [69] successfully addressed the challenge of synthesizing siloxene nanosheets by employing a scalable topological exfoliation approach. In their study, the researchers introduced amino modifications to the siloxene

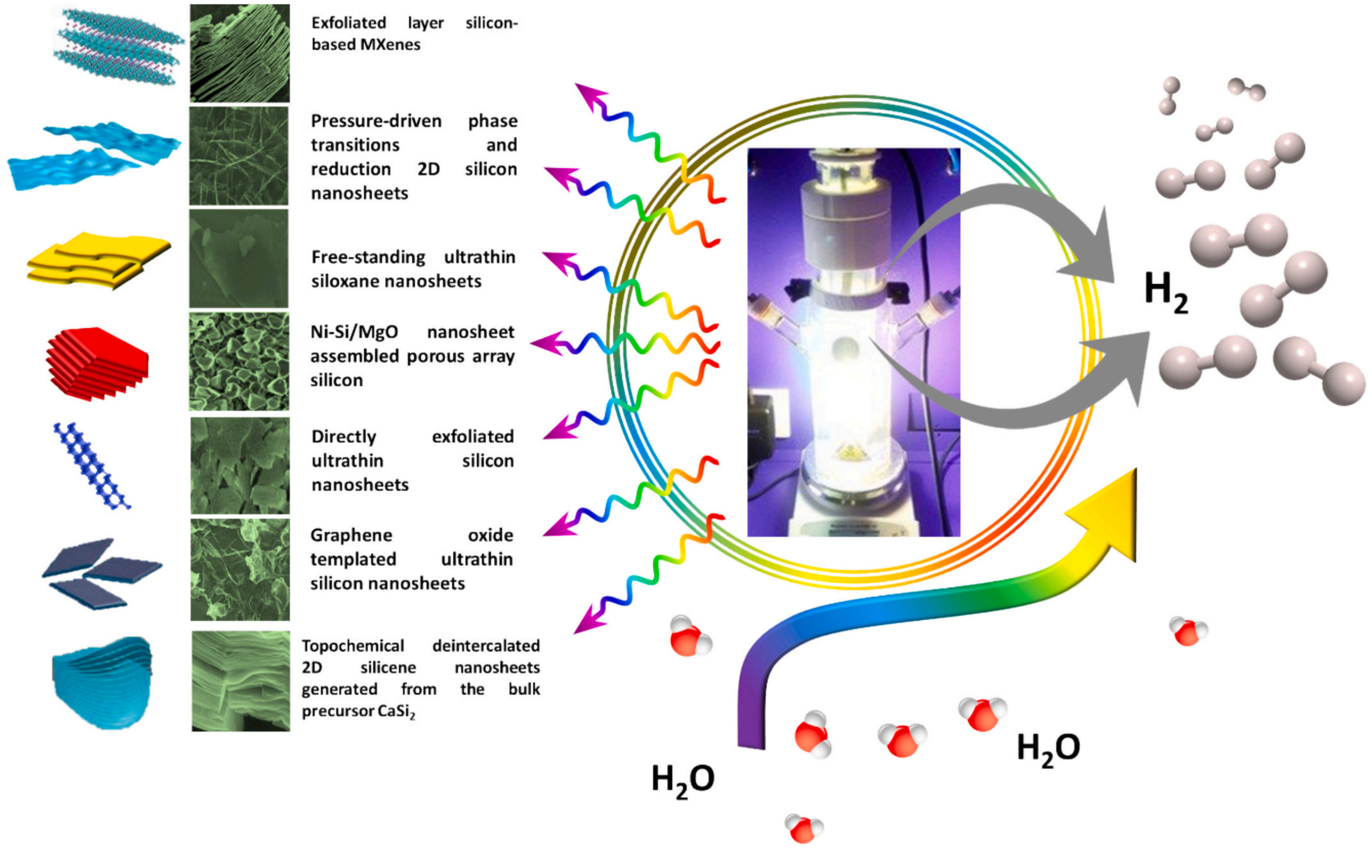

Fig. 8. The different types of nanosheet silicon composites reported by several authors [60–67].

nanosheets, which proved to be effective in carrier separation. The amino-modified siloxene nanosheets exhibited several advantages, including narrowing the bandgap of siloxene and possessing the superior structure of two-dimensional material. These modifications enhanced carrier separation, leading to a significant improvement in hydrogen production efficiency. Under simulated sunlight, the amino-modified siloxene nanosheets demonstrated a hydrogen production efficiency of over 478 % higher than that of pure siloxene. This improvement can be attributed to the unique electronic structure and suitable bandgap of the amino-modified siloxene nanosheets. Additionally, the siloxene nanosheets exhibited the capability to generate both hydrogen and hydrogen peroxide through a two-electron pathway under light irradiation, without the need for additional cocatalysts or sacrificial agents.

Li et al. [63] found that metal-free siloxene hold immense potential for efficient water splitting, a key technology for generating clean hydrogen fuel. Remarkably, unlike numerous conventional photocatalysts, siloxene exhibits exceptional hydrogen generation through photocatalytic activity without the need for additional cocatalysts or sacrificial agents. Despite its inherent instability in water, siloxene itself exhibits outstanding photocatalytic efficacy in the generation of hydrogen. Under simulated sunlight conditions, siloxene nanosheets were observed to yield an impressive 45.8 millimoles (mmol) of hydrogen per gram within the first 6 h. This yield surpasses the theoretical maximum amount of hydrogen achievable through hydrolysis by 1.13 times and exceeds the amount generated in darkness by a remarkable 6.76 times. Furthermore, the study revealed a maximum rate of hydrogen generation, reaching a noteworthy 11.4 mol (mol) per gram per hour. This exceptional result underscores the significant potential of siloxene nanosheets as a promising semiconductor for water splitting and hydrogen evolution. A critical factor contributing to the remarkable photocatalytic properties of siloxene lies in its π-conjugated electronic structure, analogous to graphene [70]. This specific electronic structure plays a crucial role in facilitating molecular charge-transfer transitions, which are vital for photocatalytic reactions. Therefore, the unique π-conjugated electronic structure of siloxene positions it as a highly favorable candidate for photocatalytic reactions, particularly in the context of hydrogen evolution.

The advantageous properties of two-dimensional (2D) silicon-based nanosheets have been extensively exploited in recent photocatalytic research due to their high surface-to-volume ratio, tunable electronic characteristics, and enhanced charge carrier dynamics. These materials have been demonstrated to promote efficient charge separation and migration, which are critical for minimizing recombination losses and maximizing photocatalytic hydrogen (H_2) evolution. It has been recognized that ultrathin silicon nanosheets, owing to their high surface area and reduced thickness, facilitate the rapid transport of photogenerated charge carriers to active sites. Enhanced photocatalytic efficiency has also been attributed to the introduction of hierarchical porosity, which improves light absorption via internal reflection and increases the availability of catalytic sites. Such morphological features have been reported to significantly outperform traditional nanorod structures. Silicon nanosheets synthesized through molten salt-assisted exfoliation and chemical reduction, as suggested by Ryu et al., have shown superior photocatalytic activity, especially when combined with noble metal cocatalysts such as platinum. This synergy has resulted in a substantial increase in hydrogen evolution rates under visible light, highlighting the role of cocatalyst-induced charge separation enhancement. Recent advances in surface functionalization, such as amino-modification of siloxene nanosheets, have been shown to effectively narrow the bandgap and improve electron-hole separation, thus markedly boosting photocatalytic activity. Interestingly, metal-free siloxene nanosheets have also demonstrated intrinsic photocatalytic activity without the requirement for sacrificial agents or cocatalysts, attributed primarily to their π-conjugated electronic structure. Particular attention should be given to strategies that enhance structural stability in aqueous media while preserving high photocatalytic efficacy under solar irradiation.

4.3. Silicon nanowire composite

Silicon nanowire (SiNW) arrays have gained significant attention due to several attractive features. SiNW arrays offer a large semiconductor/electrolyte interfacial area, which is beneficial for diverse applications for instance, photovoltaics, sensors, and energy storage devices. The increased interfacial area allows for enhanced interaction between the semiconductor and the surrounding environment [71]. Additionally, SiNW arrays exhibit an enhanced light scattering effect, which can be advantageous for photovoltaic applications. The scattering of light within the nanowire array increases the optical path length, leading to improved light absorption and overall device efficiency. SiNWs also display efficient transport of charge carriers. The unique one-dimensional structure of nanowires enables fast electron and hole transport along the wire axis, reducing the recombination rate and improving the overall device performance.

One of the significant advantages of SiNWs is their wider band gap compared to bulk silicon. This is primarily attributed to the quantum confinement effect, which occurs when the dimensions of the nanowire approach the scale of the electron's wavelength. Both first principle calculations and experimental results have confirmed the widening of the band gap in SiNWs [72,178]. A transition from an indirect to a direct band gap can be undergone by silicon nanowires (SiNWs) with diameters in the nanometer range. The significance of this transition lies in the heightened efficiency observed in light absorption and emission processes in direct band-gap materials, rendering SiNWs promising for applications in optoelectronics. The performance of various SiNWs and other silicon-based systems in the electro-catalytic generation of hydrogen is presented in Table 1. In the study reported by Ning et al. [72,178], ultralong porous SiNW arrays were synthesized using the metal-assisted anodic etching (MAAE) method. The high hydrogen (H_2) production rate observed in SiNWs is attributed to their large specific surface area and intrinsic strain in the wire. These factors facilitate the reaction between Si and water, leading to increased H_2 generation. In a study by Lu et al. [89], silicon nanowire (SiNW) arrays were co-doped with TiO_2 on FTO substrate. This co-doping was achieved through a two-step process. During hydrothermal growth, rutile TiO_2 nanowires were formed on the FTO substrate. Subsequent treatment with H2S led to the release of silicon (Si) from the conductive glass. This released Si was then incorporated into the TiO_2 lattice, resulting in co-doped SiNW arrays. This innovative doping technique presents an intriguing possibility. By tailoring the co-doping parameters, the properties of the resulting SiNW arrays can potentially be customized, expanding their applicability in the field of photocatalysis.

A recent study by Nguyen et al. [90] investigated the fabrication of TiO2-coated silicon nanowire (SiNW) arrays using atomic layer deposition (ALD) within a vacuum chamber. The researchers aimed to investigate the solar water-splitting properties of these structures. The core/shell nanowire arrays, where the core is made of Si and the shell is made of TiO_2, exhibited enhanced photocurrent compared to planar Si/TiO_2 structures. The photocurrent was observed to be 2.5 times higher in the core/shell nanowire arrays. The core/shell structure of Si/TiO_2 nanowires provides an advantageous method for integrating the functions of silicon and titanium dioxide [91]. Through a core/shell configuration, the researchers strategically combined these materials, leveraging their unique properties to synergistically enhance overall performance. The synthesis of these asymmetric Si/TiO_2 core/shell nanowire structures typically involves a combination of fabrication techniques. Silicon nanowires (SiNWs) serve as the foundation for a common approach to creating high-performance photovoltaic devices. Initially, these SiNWs are synthesized using established techniques such as vapor-liquid-solid (VLS) or vapor-solid (VS) methods. Subsequently, a conformal shell of titanium dioxide (TiO_2) is selectively deposited onto one end of the SiNWs. This deposition can be achieved via various techniques like atomic layer deposition (ALD), sol-gel deposition, or chemical vapor deposition (CVD). The resulting asymmetric nanostructure exhibits a key design feature: it facilitates the effective separation of minority carriers within the semiconductors. Conversely, the majority of carriers primarily recombine at the interface between the SiNW and TiO_2 shell. This selective manipulation of carrier dynamics, characterized by separation and recombination, ultimately contributes to the enhanced performance of the nanowire arrays in terms of solar energy conversion. Furthermore, the design principle behind this dual-bandgap configuration demonstrates the potential for broader applicability beyond the specific combination of Si and TiO2. By strategically coupling two visible-light absorbers with carefully balanced photoexcited carrier generation rates upon solar irradiation, one could potentially achieve further improvements in overall solar energy conversion efficiency.

The studies conducted by Liu et al. [92], Dong et al. [93], Lu et al. [94], and Wang et al. highlight the development of various silicon-based photocatalytic systems with enhanced performance. Liu et al. [92] focused on the synthesis of Si/TiO_2 core/shell nanowire arrays modified with Au nanoparticles (SiNWs/TiO_2@AuNPs). The SiNWs/TiO_2@AuNPs structure's photocatalytic activity was improved by adding oxygen vacancies to the TiO_2 shell. Similar findings were reported by Dong et al. [93] providing additional support for the enhanced photocatalytic activities of SiNWs/TiO_2-based systems. Lu et al. [94] utilized vertically aligned 1D SiNW arrays to create a *Z*-scheme photocatalytic device decorated with well-dispersed Co_3O_4 nanoparticles. The Co_3O_4 nanoparticles were obtained through a simple calcination procedure. The interfacial energetics analysis indicated that Co_3O_4 is a suitable material for fabricating effective Z-scheme photocatalytic devices using SiNWs. The SiNWs@$Co_3O_{4\text{–}0.3\ \mathrm{M}}$ arrays demonstrated a significantly higher H_2 evolution rate compared to bare SiNW arrays, showcasing an improvement of more than threefold. Drawing inspiration from previous research, Wang et al. [26] designed a groundbreaking solar water-splitting system. This innovative system, driven by the synergistic interplay of silicon/hematite decorated gold nanoparticles, achieves a remarkable efficiency of 6.0 % under AM 1.5G illumination, eliminating the need for an external bias. While these studies demonstrate the superior photocatalytic performance of silicon-based materials, it is important to note that the catalysts were constructed on high-purity silicon wafers. The use of high-purity silicon ensures better control over the material properties and minimizes potential impurities that could affect the photocatalytic performance. The protective layer would act like a shield and minimize performance degradation over time, leading to both higher efficiency and improved stability.

In a study by Hwang et al. [95], hierarchical Si/InGaN nanowire arrays were investigated. Notably, these structures feature InGaN nanowires, possessing diameters less than 100 nm, conformally grown upon Si wire arrays. The InGaN alloy, exhibiting a band gap of approximately 2.0 eV, presents a significant advantage for total water splitting due to its alignment with the overpotential requirements of the water oxidation reaction. Additionally, estimates by Moses et al. [96] propose that the VBM of the InGaN alloy exhibits a linear increase in energy with increasing indium composition. Based on these findings, it has been hypothesized that an InGaN alloy with up to 50 % indium composition could allow for spontaneous overall water splitting. The CBM and VBM of the InGaN alloy both meet the energy requirements for water splitting. InGaN nanowires exhibit increased minority carrier diffusion lengths and excellent absorption coefficients for visible light [97]. The ideal bandgap characteristics and energetic alignment of the CBM and VBM in InGaN alloy nanowires, with the appropriate indium composition, hold the potential for effective overall water splitting. These discoveries pave the way for the development of efficient photoelectrochemical systems for water splitting and related applications. The unique properties of GaN and alloy nanowires, particularly InGaN, offer opportunities for harnessing solar energy for sustainable hydrogen

Table 1
shows the performance of different SiNW and other silicon-based systems.

Material	Shape	Preparation method of silicon nanostructures	Photovoltage (V)	Sweep Rate (mVs^{-1})	Electrolyte	Significance of enhanced H_2 production	Ref
Pt/SiNW	NWs	metal-catalyzed electroless etching	0.42	100	H_2SO_4 + 0.5 M K_2SO_4	This enhancement was attributed to the combination of factors, including the extremely high surface roughness of SiNWs, a positive shift in the flat band potential (EFB), and light-trapping enabled by the low reflectance of SiNWs.	Oh et al. [74a]
pn^+-Si/Ti/NiP_2	NWs	Deposition and calcination	0.41	50	0.5 M H_2SO_4	The reasonable optical transparency and electrocatalytic activity of the NiP_2 cocatalyst, coupled with the intimate semiconductor/cocatalyst interface, resulted in enhanced PEC performance and durability.	Chen et al. [74b]
MoS_3 /SiNW	NWs	The metal-catalyzed electroless etching method	+0.10	1	H_2SO_4 + 0.5 M K_2SO_4	The development of a bio-photoelectrochemical cell for sustainable hydrogen production using a MoS3-modified Si nanowire photocathode and a microbially catalyzed bioanode. The integration of these components enables efficient utilization of solar energy and improves hydrogen production performance.	Zang et al. [73]
TiO_2/Pt/SiNW	NWs	Etching and Atomic Layer Deposition process	0.65	–	0.5 M H_2SO_4	The SiNW arrays decorated with Pt nanoparticles and passivated with the TiO_2 layer demonstrate superior photoelectrochemical performance compared to planar Si, Pt/planar Si, and TiO_2/Pt/planar Si photoelectrodes. This indicates the effectiveness of the SiNW architecture combined with Pt decoration and TiO_2 passivation in enhancing the overall performance of the photoelectrode.	Li et al. [70]
Si-NWs/Co-B	NWs	Electroless plating	0.87	10	Phosphate buffer solution	The enhanced PEC H_2 production of M-B modified Si-NW arrays is attributed to the excellent electrocatalytic properties of Ni—B and Co—B catalysts in a neutral solution. The uniformly distributed M-B NPs along the sidewalls of each Si-NW in the array play a crucial role in reducing the resistance at the photocathode/electrolyte interface compared to that of the bare Si-NW array. This reduced resistance facilitates a higher photocurrent response and faster H+ reduction, leading to improved H2 production efficiency.	Yang et al. [74]
SiW@MoS	NWs	Electrodeposition procedure	−0.2	2	1.0 m Na_2SO_4	The lower efficiency of the Si-NW@MoS_2 system is attributed to the poor photoelectrochemical activity of the native Si-NW electrode. To enhance efficiency, the authors suggest introducing a thin n + -Si layer on top of the nanowire to create a pn junction, which would improve charge separation within the silicon nanowire.	Tran et al. [75]
Ru/SiNW	NWs	Etching and layer deposition	− 0.18	5	0.5 M H_2SO_4	SiNWs modified with an appropriate content of Ru nanoparticles hold promise as an electrocatalyst for the hydrogen evolution reaction (HER). The enhanced electrocatalytic activity of Ru/SiNW-42.9 compared to pure Ru particles highlights the potential of this composite for HER applications.	Zhu et al. [76]
NbS_2-Si NWs	NWs	metal-assisted chemical etching (MACE)	0.34	5	0.5 $HClO_4$	The direct deposition of 2D-NbS_2 on Si NWs improved the charge transfer characteristics at the Si-NbS_2 interfaces, leading to an enhanced turn-on potential. Specifically, the turn-on potential shifted from 0.06 V to 0.34 V vs RHE, with a current density of −28 mA/cm^2 at 0 V vs RHE. These results indicate that the 2D-NbS_2 electrocatalyst synergistically addresses the poor surface kinetics of Si, resulting in improved solar water electrolysis performance.	Gnanasekar et al. [77]
MoS_2/Si	NWs	Atomic layer deposition	~0.30	100	0.5 M H_2SO_4	The photoactivity was significantly improved in the Si NW array compared to the planar surface, indicating that increasing the surface area decreases the surface flux of electrons	Zhang et al. [78]

(continued on next page)

Table 1 (*continued*)

Material	Shape	Preparation method of silicon nanostructures	Photovoltage (V)	Sweep Rate (mVs^{-1})	Electrolyte	Significance of enhanced H_2 production	Ref
						and reduces the requirement for catalytic activity on the surface.	
Pt-Au-SiNW	NWs	Thermal evaporation oxide-assisted growth	0.17	5	0.5 M of H_2SO_4	Platinum facilitates fast hydrogen adsorption, gold aids in the rapid migration of adsorbed hydrogen atoms, and silicon contributes to a high rate of hydrogen evolution.	Jiang et al. [79]
Rh-graphene/ SiNWs	NWs	Hydrothermal method	0.046	5	0.5 M H_2SO_4	The introduction of fluorine atoms affects the electronic structure of the catalyst, resulting in a strong proton-adsorption-dominated property, which contributes to high electrochemical performance and excellent stability.	Shen et al. [80]
WS_2/nano-Si etched	Nano silicon	Ball milling	0.045	5	0.5 M of H_2SO_4	The significant reduction in the activation barrier of automatic dissociation on silicon nanostructures and the formation of a complex comprising hydrogen (—H) and hydroxyl (-OH) components from the nanostructured silicon.	Ensafi et al. [81]
Rh-SiQD-GQD	QD	Electrolytic etching method	0.3	5	0.5 M of H_2SO_4	The addition of carbon quantum dots (CQDs) played a crucial role in preventing the aggregation of Rh nanoparticles, providing anchor sites, and enhancing the rate of charge transfer.	Dang et al. [82]
PdCu-silica-CNT system	Nano silicon	Chemical method	0.3	5		The PdCu/SBA-15-MWCNT-CPE exhibited a small Tafel slope (45 mV dec^{-1}), low onset potential (∼ − 150 mV), high current density (−165.24 mA cm^{-2} at −360 mV), and exchange current density (2.51 mA cm^{-2}), along with excellent durability for HER in H_2SO_4 solution.	Chiani et al. [83]
Porous silicon-Pt-Pd/Ru/Rh	–	Electroless Ag deposition	0.25	5	0.5 M of H_2SO_4	Pt/PSiF exhibited an excellent HER activity with a Tafel slope of 46.9 mV dec − 1, similar to commercial Pt/C catalysts, suggesting that the inclusion of the exfoliated graphene oxide layer further improved the catalytic performance.	Ensafi et al. [84]
$Fe_xNi_{100-x}O_y$/Si	–	Electroplating	0.05	5	0.1 M KOH and NaOH electrolytes over LiOH	The two-sided FexNi100–xOy/Si electrode could enhance hydrogen production, achieving a maximum H_2 efficiency of 140 %. This efficiency includes both Faradaic H_2 production (direct electrochemical reaction) and non-Faradaic H_2 evolution through Si corrosion (indirect reaction).	Perez Bakovic et al. [85]
Carbon cloth/ TiC/Pt,	–	atomic layer deposition (ALD)	0.03	1	1 M KOH or 0.5 M H_2SO_4	Increasing the thickness of the Pt layer beyond 3 nm showed minimal improvement in catalytic performance on CC/TiO2, while 8 nm Pt on CC/TiC exhibited slightly better activity. However, considering cost considerations further investigation of catalyst stability needs to be performed.	Gao et al. [86]
RhSi	Nanocatalyst	solvothermal method	0.054	5	0.5 M H_2SO_4	TiSi materials with the space group P213, if the (210) facet (corresponding to the strongest XRD peak) is used, the barrier of FeSi (1.58 eV) is not as low as other MSi, suggesting that the (210) facet may not be responsible for the observed electrochemical properties. Additionally, although the barrier for CoSi (210) is very low, the ΔG is not ideal.	He et al. [87]
Novel 13× Zeolite/ PANI	Nanocatalyst	hydrothermal method.	−0.274	2	0.5 M H_2SO_4	The 13X zeolite/PANI-15 composite electrode exhibited excellent catalytic performance, as demonstrated by low overpotentials at 10 mA cm^{-2} for HER and 20 mA cm^{-2} for OER. These results indicate the electrode's effectiveness in facilitating the respective electrochemical reactions.	Vinodh et al. [88]

production through water-splitting processes.

One application where the activity of MoS_2 has been explored is in photocathode systems using silicon (Si) nanowire (NW) arrays as a model [98,99]. The design involves the integration of MoS_2/TiO_2/Si NWs in a well-defined coaxial heterostructure as the photocathode. This study highlights the outstanding performance of the Si/InGaN nanowire array, with a maximum photocurrent density of 15 mA/cm^2 at 0 V vs. RHE, signifying its potential for efficient solar energy conversion. This exceptional performance surpasses typical single-component structures. Furthermore, the system demonstrates noteworthy stability under the specified operating conditions. Density functional theory (DFT) computations have also contributed to our understanding of the photocatalytic properties of Si NWs, in addition to experimental studies. As demonstrated by computational studies by Sk et al. [100], silicon nanowires (SiNWs) harboring a co-adsorbed surface coverage of hydrogen (H) and chlorine (Cl) exhibit promising potential as photocatalysts for solar-driven water splitting. This tandem surface modification bestows upon the SiNWs concurrent reducing and oxidizing capabilities, crucial for facilitating both hydrogen evolution and oxygen evolution reactions during water splitting. Notably, the presence of Cl atoms plays a pivotal role in suppressing electron-hole recombination, a detrimental process that hinders photocatalytic efficiency. This suppression is achieved through a strategic spatial separation of the HOMO and LUMO distributions, effectively preventing detrimental recombination events.

The unique structural features of silicon nanowires (SiNWs) make them highly promising for a wide range of applications, particularly in photocatalysis and solar energy conversion. The increased surface area offered by SiNW arrays enhances semiconductor/electrolyte interactions, facilitating efficient charge carrier transport, which is critical for photocatalytic processes. The one-dimensional architecture of SiNWs significantly reduces recombination losses by allowing rapid electron and hole transport along the wire axis. Various modifications to SiNW structures, such as co-doping or the formation of core/shell nanowires, have been demonstrated to enhance photocatalytic activity by tailoring the material's electronic properties. These strategies promote efficient charge separation, which is key to improving overall photocatalytic performance. The integration of SiNWs with other materials, such as gold nanoparticles or cobalt oxide, has further been shown to boost hydrogen evolution rates, confirming the potential of these composites for hydrogen production. The hierarchical Si/InGaN nanowire arrays suggest that combining materials with complementary electronic properties can lead to systems capable of achieving overall water splitting.. Future research should focus on improving the material durability and enhancing the control over the electronic properties of SiNWs to further advance their applicability in clean energy technologies.

4.4. Silicon carbide/nitride photocatalyst

Silicon carbide (SiC) has excellent physical and chemical properties that make it attractive for various engineering applications. In recent years, researchers have focused on enhancing the performance and durability of SiC photocatalysts using unique SiC nanostructures. These nanostructures, such as quantum dots, offer several advantages due to their unique size-dependent properties [14]. SiC quantum dots, for example, have a high surface-to-volume ratio, which increases the active sites available for photocatalytic reactions. They can also exhibit size-dependent optical properties, enabling control over the absorption and emission of light. Silicon carbide (SiC) quantum dots exhibit properties that render them highly promising candidates for applications like water splitting, a process harnessing solar energy to convert water into hydrogen fuel [14]. Since the pioneering explorations of water splitting in 1990, researchers have embarked on a continuous quest to optimize the performance and durability of SiC photocatalysts through diverse engineering strategies. These strategies often involve the synthesis of SiC nanostructures with controlled sizes, shapes, and compositions to optimize their photocatalytic properties. The utilization of SiC nanostructures, including quantum dots, in SiC photocatalysts has opened new possibilities for improving their efficiency and longevity, expanding their potential applications in areas such as solar energy conversion, water purification, and environmental remediation.

The SiC-graphene nano heterojunction combines silicon carbide (SiC) and graphene materials in a heterostructure arrangement. The close interfacial contacts between SiC and graphene facilitate improved charge separation and transfer [101]. The formation of Schottky-junction interfaces within the nano heterojunction enables effective charge separation, resulting in increased photoactivity for water splitting. The SiC-graphene nano heterojunction holds the potential for utilizing light energy to drive the water-splitting reaction and generate hydrogen as a sustainable and clean energy source. Similarly, the CNTs/SiC nanowire nano heterostructures involve the combination of carbon nanotubes (CNTs) and SiC nanowires [102]. Precipitation techniques are employed to fabricate these nano-heterostructures, resulting in the formation of straight silicon carbide (SiC) nanowires and intricately curved carbon nanotubes (CNTs). Coaxial core-shell nanotubes (C@SiCNTs) are constructed by uniformly coating the CNTs with SiC nanoshells through an in-situ vapor-solid reaction, as reported in [103]. This judicious configuration, characterized by a coaxial core-shell structure, fosters the formation of tightly coupled Schottky junctions at the interface between the CNTs and SiC. This, in turn, enhances both interfacial coupling and charge separation within the nano-heterostructures. The improved charge separation translates to a significant amplification in photocatalytic performance, particularly evident in the efficient generation of hydrogen (H_2) from pure water. The investigations by Jian et al. [104] highlighted the potential of these designed nano heterostructures to enhance the effectiveness and performance of photocatalytic processes. Tailored nano heterostructures show promise for solar and water-splitting applications due to improved charge separation and photoactivity. They provide a pathway for developing efficient and long-lasting photocatalytic systems for clean energy generation and open up new avenues for research in this field.

The fabrication of a highly promising photocathode was achieved by Kato et al. [105] through the meticulous epitaxial growth of p-type 3C-SiC on 4H-SiC using chemical vapor deposition (CVD). This strategic approach yielded a photocathode with exceptional characteristics, paving the way for advancements in solar-to-hydrogen conversion technologies. This photocathode exhibited potential for efficient water reduction, and its performance was further enhanced by the application of Pt nanoparticles. An initial solar-to-hydrogen (STH) conversion efficiency of 0.52 % was achieved. This initial value serves as a baseline for subsequent optimization efforts. Furthermore, the strategic incorporation of a Pt-coated 3C-SiC p-n junction photocathode led to a commendable increase in STH efficiency, reaching 0.72 %. This significant improvement warrants a closer scientific examination to elucidate the underlying mechanisms responsible for the enhanced performance. These findings underscore the potential efficacy of p-type 3C-SiC in facilitating efficient water reduction processes. While n-type 3C-SiC exhibits promising characteristics for various applications, its utilization as a photoanode for the photoelectrochemical (PEC) water oxidation process presents distinct challenges. This discrepancy arises from the inherently different characteristics of the oxidation and reduction reactions involved. Considerable promise for various applications is exhibited by n-type 3C-SiC. However, substantial hindrances are encountered in its utilization as a photoanode for photoelectrochemical (PEC) water oxidation. These hindrances emanate from elevated energy barriers, posing significant challenges to the attainment of efficient and sustainable water splitting. A closer scientific examination is necessitated to illuminate the fundamental limitations and pave the way for potential solutions.

To overcome these challenges, researchers are actively exploring various strategies. One approach is the development of novel materials that can enhance the water oxidation kinetics and improve the charge transfer processes at the photoanode surface. This involves the design and synthesis of materials with tailored electronic band structures and catalytic properties to facilitate the water oxidation reaction. Nano structuring techniques are also being investigated to create high-surface-area photoanodes, which can increase the active sites for water oxidation. By increasing the surface area, more photoelectrons can participate in the water oxidation reaction, improving the overall efficiency. In addition, nano structuring surface modifications and functionalization methods are being explored to enhance the catalytic activity and stability of n-type 3C-SiC photoanodes [14]. These modifications can include the deposition of co-catalysts, surface coatings, or doping with specific elements to enhance charge transfer and catalytic properties. Addressing the limitations in the water oxidation process is crucial for advancing the field of PEC water splitting. By improving the performance of n-type 3C-SiC photoanodes, researchers aim to achieve efficient and scalable hydrogen production from renewable sources. Continued research and development efforts in this area hold promise for unlocking the full potential of PEC water splitting as a clean and sustainable method for hydrogen generation.

One approach is to coat the photoanodes with protective layers or nanoparticles. For example, promising strategies have been demonstrated in scientific studies aimed at enhancing the photoelectrochemical (PEC) performance and stability of n-type 3C-silicon carbide (SiC) photoanodes for water oxidation. The work by Song et al. [106] exemplified that the application of Pt nanoparticles onto n-type 3C-SiC photoanodes substantially augments their PEC performance and provides protection against photo corrosion. This nanoparticle coating functions as a protective layer, averting the degradation of the photoanode surface and ensuring its stability during extended operational periods. The balanced integration of efficient oxygen evolution reaction (OER) cocatalysts onto 3C-SiC emerges as a promising strategy for amplifying water oxidation performance and ameliorating the stability of photoanodes. This synergistic approach warrants a closer scientific examination to shed light on the underlying mechanisms driving its effectiveness. Investigations conducted by Jian et al. [107] meticulously explored the impact of various oxygen evolution reaction (OER) cocatalysts on the water oxidation performance of 3C-SiC. Their findings revealed a significant enhancement in performance upon the deposition of diverse cocatalysts, including nickel oxide, iron oxyhydroxide (FeOOH), and nickel-iron oxyhydroxide (Ni:FeOOH). This study warrants a closer scientific examination to illuminate the underlying mechanisms responsible for this observed improvement. These cocatalysts facilitate the OER process and ameliorate charge transfer kinetics, ultimately resulting in heightened PEC performance. Notwithstanding these advancements, the achieved photocurrent density (Jph) with modified 3C-SiC photoanodes remains circumscribed. As reported by Jian et al. [107], an impressive peak photocurrent density (Jph) of approximately 1.1 mA cm^{-2} was observed under AM 1.5G illumination with an intensity of 100 mW cm^{-2}. This remarkable achievement was attained at a potential of 1.23 V versus the reversible hydrogen electrode (VRHE). This underscores the imperative for further research and development to optimize 3C-SiC photoanodes for efficient and sustainable water splitting. Further research and development efforts are needed to enhance the efficiency of 3C-SiC photoanodes and approach their theoretical performance limits. Another factor that can limit the performance of 3C-SiC photoanodes is the smoothness of the as-grown planar surface. The smooth surface can result in the reflection of a portion of the incident sunlight, leading to reduced light absorption and photoconversion efficiency [108]. Improving the light-harvesting efficiency by addressing surface smoothness is crucial for enhancing the performance of 3C-SiC photoanodes in PEC water splitting. Researchers are exploring surface engineering techniques, such as nano-structuring or surface texturing, to increase light absorption and enhance the overall efficiency of 3C-SiC photoanodes.

The investigation into the influence of noble metal nanoparticles on hydrogen (H_2) production from a 3C-SiC film was conducted by He et al. [109]. An enhancement in photocurrent for a Si-based photocathode coated with 3C-SiC was observed under specific conditions of metal nanoparticle deposition in their study. The observed augmentation was meticulously ascribed to plasmonic effects, well-recognized for their remarkable ability to bolster light absorption and the generation of charge carriers. In a separate study, a photocathode utilizing an n-type 3C-SiC/p-type Si heterojunction was employed by Han et al. [110]. The formation of an efficient heterojunction solar cell on a silicon (Si) substrate was facilitated by harnessing the intrinsic properties of 3C-SiC, including its high electron affinity (4.0 eV) and band gap (2.3 eV). This configuration effectively suppressed minority carrier injection from the Si substrate, ultimately resulting in heightened device performance. The photocatalytic properties of GeC/SiC hetero-bilayer for hydrogen (H_2) generation through water splitting were investigated by Islam et al. [111] utilizing density functional theory. Highlighted the potential of GeC/SiC structures for H_2 fuel generation. Further studies to engineer the intrinsic content of the GeC/SiC vdW-HBL to enhance its photocatalytic and photo-absorption properties. Suggested exploring optical and electronic properties of the vdW-HBL in response to changes in stacking patterns or the incorporation of biaxial strain as important strategies for enhancing its photocatalytic activities.

Scientists investigated how adding a tiny amount of nitrogen to a material called silicon carbide could make it better at producing hydrogen fuel from sunlight [112]. Simulations indicated that the performance of 3C-SiC could be improved through N-doping in comparison to other SiC-based photocatalysts for H_2 generation. Experimental validation substantiated the simulations, with N-doped 3C-SiC demonstrating a remarkable H_2 production rate of 205.3 μL/g-h. This achievement signifies a substantial enhancement when contrasted with undoped SiC-Ar (120.1 $\mu L/g^{-h}$) and outperforms other frequently studied SiC-based photocatalysts. Incorporating nitrogen into SiC results in the introduction of various parameters that improve photocatalytic activity. First, the adjustment of the bandgap and carbon surface enhances the light absorption ability of the material, allowing for increased utilization of solar energy. Second, the efficient separation of photo-excited carriers at the interface plays a crucial role in preventing recombination and maximizing the utilization of generated charge carriers. This separation is facilitated by the presence of the N-dopant. Furthermore, the presence of hole traps, defects, and grain size can contribute to the chemical activities of the photocatalyst, leading to enhanced performance. Lastly, the enhanced photocatalytic performance of N-doped 3C-SiC is further attributed to the heightened light absorption induced by the presence of carbon, emanating from the phase transformation process during N-doping. In a broader perspective, analogous enhancements are observed within other classes of photocatalysts. (Oxy)nitrides, comprising photocatalysts incorporating transition metals such as Ti^{4+}, Nb^{5+}, and Ta^{5+}, similarly exhibit improved performance upon the inclusion of nitrogen. This incorporation results in the hybridization of N 2p and O 2p orbitals, notably pronounced in the valence band. Due to the greater contribution of N 2p orbitals, the overall bandgap narrows compared to pure oxides. This reduction in bandgap positions (oxy)nitrides as highly promising candidates for high-performance photoanodes, capable of efficiently harvesting a broader spectrum of solar light.

The incorporation of SiC nanostructures, including quantum dots and heterojunctions, has been investigated extensively to enhance their photocatalytic performance. SiC quantum dots exhibit a high surface-to-volume ratio, which increases active sites for photocatalytic reactions, enabling better light absorption and more efficient energy conversion. The combination of SiC with materials like graphene and carbon nanotubes (CNTs) in nano-heterostructures has been shown to improve charge separation and transfer, thereby enhancing photocatalytic activity. The formation of Schottky-junction interfaces in SiC-based heterostructures has facilitated increased photoactivity, particularly for water splitting reactions. The creation of well-structured SiC/graphene and CNT/SiC nanowires has demonstrated efficient hydrogen generation. The integration of Pt nanoparticles onto SiC photocathodes has been proven to further enhance the solar-to-hydrogen conversion efficiency, supporting the use of SiC in solar-driven water reduction processes. The N-doped 3C-SiC material exhibited a remarkable increase in hydrogen production rate, which was attributed to modifications in its electronic structure and light absorption properties. The introduction of nitrogen reduces the bandgap of SiC, enhancing its ability to capture a broader spectrum of sunlight and improving charge carrier separation. This doping technique, along with other strategies like the deposition of cocatalysts or the fabrication of protective layers, holds the potential to optimize the photocatalytic performance of SiC. Further studies are necessary to refine these materials and address challenges related to their scalability and long-term stability in real-world applications.

4.5. *Heterostructure silicon photocatalyst*

Doping plays a crucial role in modifying the properties of semiconductor photocatalysts and enhancing their photocatalytic activity. By introducing dopant atoms into the semiconductor lattice, various characteristics of the material can be altered, including carrier concentration, electrical transport properties, and surface states. This modification facilitates augmented light harvesting, optimized charge separation, and expedited charge transfer dynamics, collectively culminating in an elevation of photocatalytic activity [113]. Co-doping, which involves the simultaneous introduction of multiple dopant elements, can result in synergistic effects that further enhance photocatalytic activity. For example, co-doping can lead to improved electrical conductivity and activity for specific reactions like the oxygen-evolution reaction (OER). The combined presence of multiple dopants can create unique electronic and catalytic properties that are not achievable with single doping elements alone. In the context of silicon (Si), its particles exhibit a band gap that can vary from 1.1 to 5.4 eV depending on their sizes. This study proposes a promising strategy for harnessing a broader range of the solar spectrum, suggesting that coupling silicon (Si) particles with wide-bandgap semiconductors, like titanium dioxide (TiO_2), can lead to increased absorption in the visible light region. This broader absorption range allows for better utilization of solar energy and higher efficiency in photocatalysis. A summary of Si photocatalysts for hydrogen production is shown in Table 2.

The solar-to-hydrogen conversion ratio of heterostructure photocatalysts can vary depending on several factors. Heterostructure photocatalysts are composed of different materials that are combined at the nanoscale to create a composite with enhanced photocatalytic properties for hydrogen production from solar energy (Fig. 9). It is important to note that the performance of heterostructure photocatalysts can vary depending on the specific combination of materials, synthesis methods, fabrication techniques, and optimization strategies used. By carefully selecting and engineering the doping elements and coupling different semiconductors, researchers can tailor the properties of photocatalysts to optimize their performance for H_2 production. Strategies that enhance light absorption, charge separation, and overall efficiency in photocatalytic systems are of great importance in facilitating sustainable H_2 energy conversion.

Doping TiO_2 with Si has emerged as a promising method for enhancing the photoactivity and performance of these widely used

Table 2

Summary of Si-based heterojunction photocatalysts for hydrogen production.

Feedstock	Synthesis method	Cocatalyst	Light source	Solvent	H_2 generation rate (μmol h^{-1} g^{-1})	Ref
Metallurgical grade Si	Ball milling	– Pt	300 W Xe lamp with 420 nm cutoff filter	Water and methanol	1003.3 μmol·g^{-1}·h^{-1}	Lv et al. [38]
Rice husk-based silicon	Magnetiothermic reaction	MgO	Visible light	Water	3200 μmol·g^{-1}·h^{-1}	Islam et al. [114]
SiC	–	graphitic carbon	Visible light	water	180.2 μmol·g^{-1}·h^{-1}	Wang et al. [26]
Si powder	Cryo-exfoliation	–	300 W Xe lamp with 400 nm cutoff filter	Water and methanol	54.8 μmol·g^{-1}·h^{-1}	Wang et al. [64]
Si nanowire arrays,	etching−lithiation approach	–	Visible light	Water and lithium	6.0 μmol·g^{-1}·h^{-1}	Ma et al. [115]
Silicon Nanosheets	exfoliation procedure of Si	–	Visible light	Water and methanol10%	54.8 μmol•h-1•g-1,	Wang et al. [64]
$CaSi_2$	Topochemical	–	Not available	Water	~8988 μmol·g^{-1}·h^{-1}	Ma et al. [116]
Si	Precipitation method	TiO_2/SiO_2	UV	water-ethanol mixtures	212 μmol·g^{-1}·h^{-1}	Serafin et al. [117]
Si/	Solid phase reaction	CNTs	Visible	water	648 μmol·g^{-1}·h^{-1}	Teo et al. [118]
Diamond-wire sawing silicon waste	Metal-assisted chemical etching	Ag	300 W Xe lamp with 400 nm cutoff filter	Water and methanol	157.43 μmol·g^{-1}·h^{-1}	Li et al. [119]
Rice husk-derived silicon	Solid phase reaction	CNT	Visible light	water	815 μmol·g^{-1}·h^{-1}	Islam et al. [120]
Montmorillonite clay	Mg reduction	– Pt	300 W Xe lamp with 400 nm cutoff filter	Water and methanol	723 μmol·g^{-1}·h^{-1}	Ryu et al., [61]
Rice husk-derived silicon	Solid phase reaction	MgO	Visible light	water	714 μmol·g^{-1}·h^{-1}	Islam et al. [67]
Talc clay	Mg reduction	– Pt	300 W Xe lamp with 400 nm cutoff filter	Water and methanol	1031.62 μmol·g^{-1}·h^{-1}	Jang et al. [121]
SiO_2	magnesiothermic reduction	MgO	LED	Distilled water and methanol	4437 μmol h-1 g - 1	Curtis et al. [122]
MCM-41 (mesoporous SiO_2)	Mg reduction	–	300 W Xe lamp with 400 nm cutoff filter	Water and tri-ethanolamine	604.7 μmol·g^{-1}·h^{-1}	Sun et al., [123]
SiCl4	Reduction	–	300-W Xe lamp as the light source.	Water and methanol	882 μmol·g^{-1}·h^{-1}	Dai et al. [43]
Mesoporous SiO_2	Mg reduction	–	300 W Xe lamp with 420 nm cutoff filter	Water and methanol	1785 μmol·g^{-1}·h^{-1}	Song et al. [124]
$CaSi_2$	Precipitation	–	light	water	8988 μmol h^{-1} g^{-1}	Ma et al. [116]
Stöber SiO_2 nanoparticles	Mg reduction	–	White LED (400–800 nm)	Water and methanol	4437 μmol h-1 g - 1	Curtis et al. [122]
Magnesiothermic reduction,	Mg reduction	–	under visible light	water	1785 μmol h-1 g - 1	Song et al. [124]
$SiCl_4$	NaK reduction	–	300 W Xe lamp	Water and methanol	882.4 μmol h-1 g - 1	Dai et al. [43]
Natural clay	Solid phase reaction and precipitation	–	ultraviolet (UV)	water/methanol	723 μmol H_2 per h per g Si	Ryu et al. [61]
Natural clay	Solid phase reaction and precipitation	pt	ultraviolet (UV)	water/methanol	1031 μmol h-1 g - 1	Jang et al. [121]
Si, SiO_2, B_2O_3 and P_2O_5	Sputtering	–	500 W Xe lamp (310–750 nm)	Water and methanol	~1600 μmol h-1 g - 1	Sugimoto et al. [125]

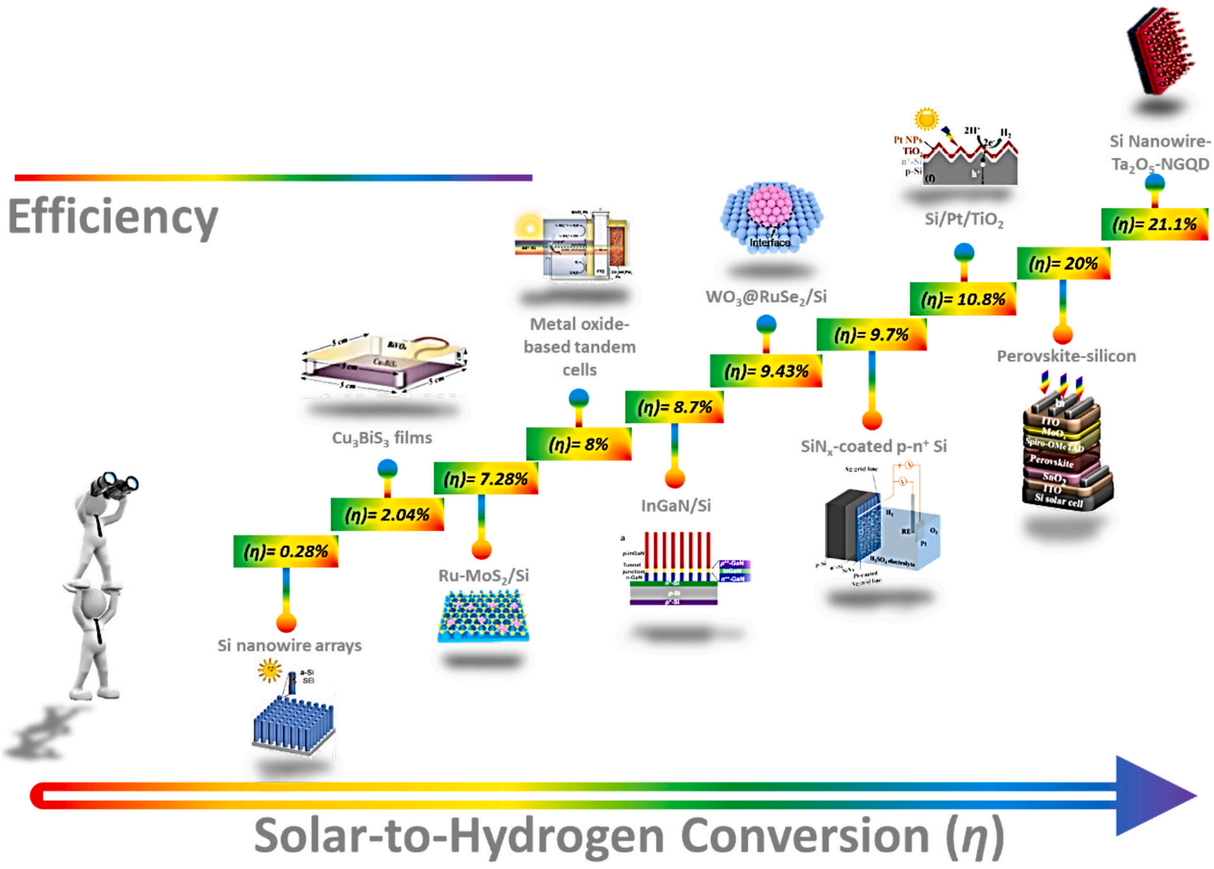

Fig. 9. The change of solar to hydrogen conversion ratio for different heterostructure photocatalysts [56,97,126–131].

photocatalysts [132]. Doping Si into the TiO_2 lattice has been found to have several beneficial effects on photocatalytic application. One of the key advantages of Si doping is its ability to increase the electron concentration and surface hydroxyl concentration of TiO_2. This increased electron concentration promotes more efficient charge transfer and separation, leading to improved photoactivity. Additionally, the higher surface hydroxyl concentration enhances the adsorption and activation of reactant molecules, further enhancing the photocatalytic performance. Si doping also influences the surface wettability of TiO_2, which can impact its photocatalytic properties. Si-doped TiO_2 surfaces have been shown to exhibit improved hydrophilicity, allowing for better interaction with water and reactant molecules [133]. This increased surface wettability enhances the accessibility of reactants to the photocatalyst's active sites, resulting in improved photocatalytic activity. The electronic band structure and electron mobility of TiO_2 can be adjusted by Si doping, as supported by theoretical calculations. Intriguingly, the integration of silicon (Si) atoms into the titanium dioxide (TiO_2) lattice alters its intrinsic electronic structure, specifically shifting energy levels and adjusting band edges. This tailored bandgap engineering enables more efficient utilization of visible light for photocatalytic applications. Furthermore, Si doping acts as a dopant, enhancing the mobility of photogenerated electrons within the TiO_2 lattice. This translates to improved transport of charge carriers and a significant reduction in recombination losses, ultimately leading to superior photocatalytic performance.

Multiple scientific studies have examined the effect of silicon (Si) doping on the photocatalytic and photoelectrochemical (PEC) properties of titanium dioxide (TiO_2). Su et al. [134] prepared Si-doped TiO_2 nanotube arrays, demonstrating improved PEC performance and highlighting the potential of Si doping in this domain. The independent studies by Jin et al. [135] and Zhang et al. [136] not only confirm the positive impact of Si doping on TiO_2 photocatalytic activity but also highlight its potential for practical applications in environmental remediation and pollutant degradation. The observed enhancements in NO reduction efficiency and charge separation open exciting avenues for developing advanced photocatalysts with improved performance. Sun et al. [137] achieved an improved visible light PEC response through the creation of Si-doped TiO_2 thin films. Dong et al. [138] fabricated Ti-Si-O nanotubes, exhibiting superior PEC activity compared to undoped TiO_2. Collectively, these studies emphasize the significant potential of Si doping in enhancing the photocatalytic and PEC performance of TiO_2-based materials. The synergistic effect of the unique one-dimensional (1D) TiO_2 nanotube structure and moderate Si doping demonstrates promising applications in improving the PEC performance of TiO_2-based photoanodes. The incorporation of Si atoms into the TiO_2 nanotube structure enhances light absorption, charge carrier transport, and surface reactions, leading to improved PEC efficiency.

A notable contribution to the field of photoelectrochemical (PEC) water splitting was presented by Zhang et al. [139] through the introduction of a novel hydrothermal method. This method facilitated the successful growth of an oriented, co-doped nitrogen (N)/silicon (Si) single-crystalline rutile TiO_2 nanorod (NR) film directly onto a transparent conductive FTO substrate. The successful co-doping of N and Si into TiO_2 represents a significant advancement in the field of photocatalysis. This augmentation resulted in a remarkable solar-to-hydrogen (STH) conversion efficiency of 1.1 %, representing the highest reported value for PEC cells utilizing TiO_2 at the time. While both N and Si doping individually improve photocatalytic activity, the co-doping strategy achieved a synergistic effect, exceeding the combined benefits of single doping. This synergy likely arises from the interplay between the modified bandgap structure, enhanced charge mobility, and optimized surface properties induced by both dopants. Co-doping effectively narrowed the bandgap of TiO_2, enabling the absorption of a broader spectrum of solar light and consequently enhancing light utilization. Co-doping induced modifications in the surface properties of TiO_2, potentially improving the adsorption of water molecules and promoting H_2 evolution reactions. Firstly, the codoping allowed for the absorption of visible light by introducing N2p states within the "forbidden gap" of TiO_2. Normally, TiO_2 can only absorb ultraviolet (UV) light, but the codoping expanded its light absorption range to include visible light, which significantly increased the available solar spectrum for energy conversion.

Further contributing to the observed performance enhancement by Zhang et al. [139] was the unique electronic structure induced by Si codoping. The introduction of Si^3s-^3p states within the TiO_2 lattice strategically localized them at the tail of the conduction band. These states played a crucial role in augmenting carrier mobility, a vital parameter for efficient charge transport in photoelectrochemical (PEC) systems. Enhanced carrier mobility translates to improved separation and utilization of photogenerated electron-hole pairs, ultimately leading to a potentiated overall PEC performance. The experimental observations were supported by rigorous theoretical calculations involving density-functional theory (DFT) and first-principles approaches. These computational simulations provided valuable insights into the modifications of the electronic structure and their subsequent impact on carrier transport behavior. These theoretical calculations confirmed that codoping TiO_2 with N and Si was more effective in improving the photoelectrochemical performance compared to mono-doping with either element alone [140]. The synergistic effects of N/Si codoping resulted in enhanced light absorption, improved carrier mobility, and ultimately, higher solar-to-hydrogen efficiency in PEC water splitting systems based on TiO_2.

To create the unique structure known as CNTs@Co@NC/D-SiO_2, Wang et al. [141] coated Co nanoparticles with N-doped carbon, encased them in carbon nanotubes and then embedded them in flawed silica. Increased photoelectric response and electrocatalytic activity resulted from this structure's improvement of the compatibility between the semiconductor and electrocatalyst interfaces. Si QDs have been researched for their potential to improve the efficiency of solar cells sensitive to quantum dots. According to Li et al. [142], Si QDs were used to modify TiO_2, which led to better visible light photoelectrochemical performance by raising the quantum yield and broadening TiO_2's light absorption spectrum. Wide bandgap semiconductors' capacity to increase photoactivity has been intensively researched concerning noble metal nanostructures like Au, Ag, or Pt. On nanoporous Si with a high Au catalyst content and appropriate photocurrents, Oh et al. [143] observed improved catalysis. Zhao et al. [144] examined nanoporous Si with a buried Pt nanoparticle layer and found that the hydrogen evolution reaction (HER) overpotential had significantly increased. However, following research by Aguiar et al. demonstrated a decline in performance after just 100 h of use, highlighting the difficulties with stability over longer time frames.

Recognizing the limitations of p-Si in photoelectrochemical hydrogen evolution (PEC-HER), Zhang et al. [145] devised a captivating solution. Their design involved a unique 3D p-Si/NiCoSe photocathode, offering a synergistic amalgamation of the light-harvesting prowess of the Si NP core and the optically transparent and electrocatalytically active NiCoSe shell. In a separate study conducted by Jin et al. [146], integrated photocathodes constructed with CoPS deposited on n^+-p-p^+ silicon micro pyramids exhibited promising outcomes. These structures generated strong photocurrents and achieved efficient solar-driven hydrogen generation using Earth-abundant materials. However, challenges persist in controlling the formation of silica nanostructures and ensuring compatibility between the semiconductor and catalyst interfaces. Further research efforts concentrated on the optimization of synthesis techniques and interface engineering are deemed crucial for addressing these limitations.

Incorporating silicon into low-dimensional carbon materials to synthesize photocatalysts for water splitting is an interesting approach that has been explored in recent years (Fig. 10). By incorporating silicon into these carbon materials, researchers aim to further enhance their properties and improve their performance as photocatalysts for water splitting. Silicon can contribute to the photocatalytic activity in several ways. First, silicon can modify the electronic structure of carbon materials, influencing their bandgap and absorption properties. This alteration has the potential to improve the absorption of light, which are crucial step in efficient water splitting. Silicon atoms act as tiny scaffolds, providing new platforms for chemical reactions to occur on the carbon surface, promoting the adsorption and activation of water molecules. The reaction kinetics can be expedited, leading to an enhancement in the overall efficiency of the photocatalyst.

Studies by Huang et al. [147] and Meng et al. [148] focused on the synthesis of composites using silicon nanowires (SiNWs) and rGO. Huang et al. fabricated SiNWs/rGO composites, which exhibited a significantly higher short-circuit photocurrent density compared to pristine SiNWs and planar Si/rGO composites. Utilizing an

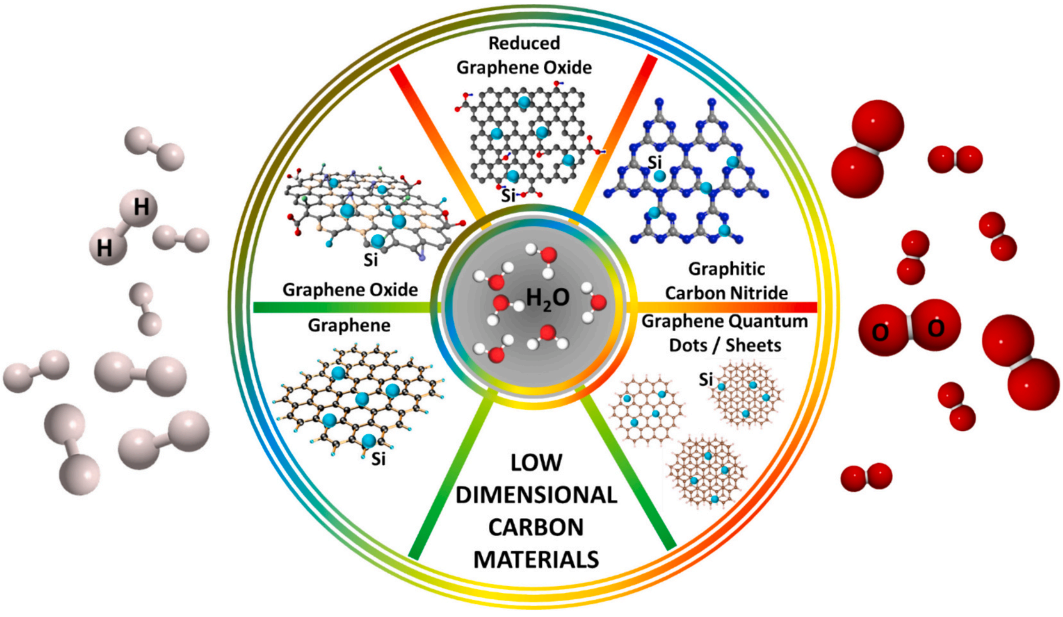

Fig. 10. The low dimensional carbon materials supported silicon photocatalyst for water splitting.

electrochemical technique, graphene oxide (GO) was directly reduced onto silicon nanowires (SiNWs) by Meng et al. [148], resulting in the successful synthesis of a SiNWs/rGO composite. This composite manifested a notable enhancement in photoelectrochemical performance, characterized by a significantly higher photocurrent density compared to bare SiNWs and a positive shift in the onset potential under illumination. The efficient charge transfer from the photoexcited SiNWs to the reduced GO (rGO), which functions as a superior conductor, is promoted by the highly interconnected network of SiNWs and rGO. This, in turn, minimizes charge trapping and recombination within the SiNWs, thereby boosting the overall photoelectrochemical activity. This augmentation further improves charge transfer efficiency and, consequently, the overall photoelectrochemical performance.

Kim et al. [149] investigated the utilization of graphene as a barrier layer to establish an electrical junction within vertically aligned silicon nanowire (SiNW) arrays. This approach aimed to modulate the overall catalytic performance. By coating SiNWs with graphene, they were able to create SiNW-graphene heterostructures that showed high sensitivity in molecular sensing applications. The presence of graphene prevented the bundling of SiNWs, allowing them to stand separately on the Si wafer. This arrangement facilitated improved electrical junction formation and enhanced performance in molecular sensing. Carbon-based nanomaterials, including graphene, have also shown promise in photoanode applications. For example, graphene-covered n-Si has been shown to enhance the stability of photoanodes in reactions such as ferrocene and bromine oxidation, as well as hydrogen reduction. While these reactions are more energetically and kinetically favorable than the oxygen evolution reaction (OER), they serve as examples of graphene's ability to improve the stability and performance of photoanodes [150]. Additionally, carbon nanotube (CNT)-graphene complexes, graphene, and graphene oxide have been investigated as electrocatalysts for the oxygen reduction reaction. CNTs have been employed to promote charge separation when combined with wide-gap semiconductor photocatalysts, further enhancing their photocatalytic activity.

The application of polymer-supported graphene to enhance the photocatalytic hydrogen evolution reaction was investigated by Xu et al. [151]. The study revealed that graphene plays a dual role, functioning as both an electron acceptor and a site for hydrogen evolution. This dual functionality facilitates the separation of photo-induced charge carriers, ultimately promoting increased efficiency in hydrogen production. In a distinct study conducted by Bae et al. [152], graphene layers were effectively deposited onto GaN nanowires (GaN NWs) to act as a protective layer and enhance electron transfer for water splitting. The resulting graphene-coated GaN NWs (Gr/GaN NWs) demonstrated a remarkable improvement in solar-to-hydrogen (STH) efficiency, surpassing the performance of bare GaN NWs by 67 %. The graphene layer acted as a thin-film protective barrier, providing superior stability to the GaN NWs and resulting in improved performance for photoelectrochemical (PEC) water splitting. These findings highlight the potential of graphene as both a catalytically active component and a protective layer in semiconductor-based PEC water-splitting systems. Incorporating graphene can enhance the stability of composite catalysts and improve the efficiency of photocatalytic hydrogen production. However, further research is still needed to fully explore and understand the complete potential of graphene-based composite catalysts in this application.

Huang et al. [147] produced reduced graphene oxide (rGO) via a solvothermal technique and spin-coated it onto silicon nanowires (SiNWs) to enhance H_2 generation. Because of its straightforward transfer, chemical stability, and oxidation resistance, chemical vapor deposition (CVD)-grown graphene is preferred. Sim et al. (2015) developed N-doped graphene quantum sheets as cocatalysts on SiNWs via chemical vapor deposition, which resulted in noticeably increased photocatalytic hydrogen production activity. Fellahi et al. [153] increased the photoelectrochemical (PEC) activity on SiNWs by reducing graphene oxide (GO) with UV irradiation and using it as an effective co-catalyst. However, the techniques for manufacturing rGO on SiNWs entail time-consuming preparation procedures, the waste of resources and energy, and the application of potentially hazardous materials that could damage the environment. Meng et al. [148] however, revealed an eco-friendly and less complicated electrochemical technique to directly convert graphene oxide (GO) onto SiNWs. With a considerably larger photocurrent density compared to bare SiNWs and a favorable shift in the onset potential under illumination, the resulting SiNWs/rGO photocathode demonstrated better PEC performance. These improvements are attributed to the heightened electrical conductivity of reduced graphene oxide (rGO) and the enhanced separation of photogenerated charge carriers.

The doping of silicon (Si) into various semiconductors, such as titanium dioxide (TiO2), has demonstrated significant improvements in photocatalytic and photoelectrochemical (PEC) activities. Si doping has been shown to increase electron concentration and surface hydroxyl concentration, which in turn promotes more efficient charge transfer and separation, ultimately improving photocatalytic activity. Additionally, Si doping influences the electronic structure of TiO2, shifting energy levels and adjusting band edges, thereby expanding the material's ability to absorb visible light. The incorporation of Si atoms into the TiO2 lattice results in enhanced mobility of photogenerated electrons, reducing recombination losses and leading to superior photocatalytic performance. Furthermore, co-doping, such as the simultaneous introduction of nitrogen (N) and silicon (Si) into TiO2, has been demonstrated to induce synergistic effects that extend the material's light absorption capabilities into the visible spectrum, significantly enhancing its solar-to-hydrogen (STH) conversion efficiency. Co-doping has been found to narrow the bandgap, enhance carrier mobility, and optimize surface properties, further improving PEC performance. The integration of Si into low-dimensional carbon materials, such as graphene and silicon nanowires (SiNWs), has been explored to enhance photoelectrochemical performance by improving light absorption and charge transfer efficiency. Despite these promising developments, challenges related to material stability and the optimization of synthesis methods remain, highlighting the need for further research to fully exploit the potential of Si-doped photocatalysts in sustainable energy conversion.

4.6. *Metal-organic framework with silicon*

By controlling the potent interaction between metal ions and ligands, conductive MOFs can be made. Conductive MOFs enable better electrocatalytic performance by providing effective mass transport and simple access to active sites. Silicon-containing organic compounds, such as organosilanes or organosilicates, can serve as ligands in the synthesis of silicon-based MOFs (Fig. 11). These compounds contain both organic groups and silicon atoms, allowing for the integration of silicon into the MOF framework. The presence of silicon in the ligands can introduce additional functionalities and properties to the resulting MOF material. The synthesis of silicon-based MOFs typically involves the reaction between metal ions or clusters and silicon-containing ligands. These ligands can be designed to possess specific functional groups that can coordinate with the metal centers, leading to the formation of the desired MOF structure.

A polymer based on methyl viologen was employed as a redox mediator to promote effective electron transport to the electrode [166]. However, it led to a reduction in the driving force needed to activate a catalyst for H_2 evolution [167]. A perylene-diamide derivative-modified nanostructured pSi photocathode (PDI') was used in the tandem PEC system. A one-electron reduced shuttle is created when the PDI', a very electron-deficient excited state, mediates an electron transfer. By successfully activating the H_2 evolution catalyst, this process enables effective hydrogen synthesis. The construction of TiOCrIII metal-oxo clusters on the silica surface of MCM-41, a mesoporous silica material, was reported by Zhao et al. [168]. This arrangement produces visible-

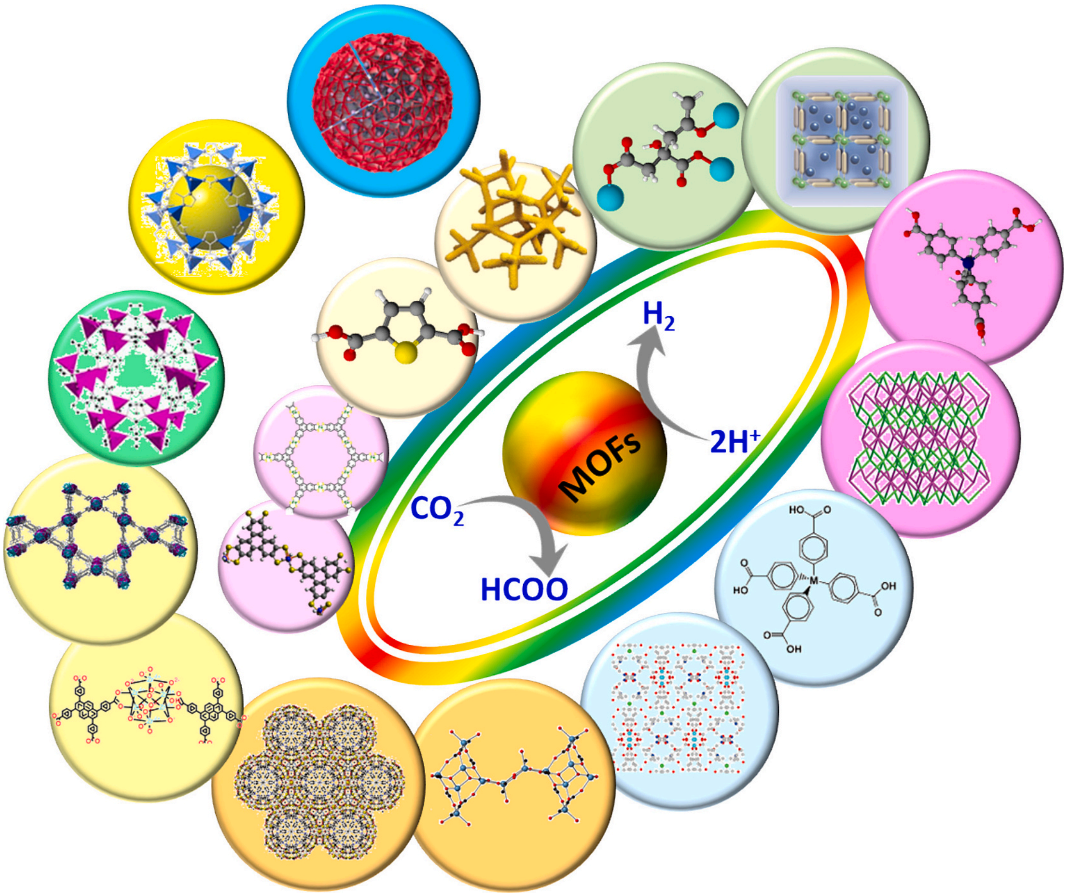

Fig. 11. Different Silicon-containing organic compounds to synthesize the silicon-based MOFs [138,154–165].

range absorption-exhibiting hetero-binuclear metal-to-metal charge-transfer chromophores. The ability to capture visible light energy, which is essential for solar energy conversion applications, is a benefit of these chromophores.

A landmark achievement in the field of water splitting has been the recent development of a cobalt-phosphate (Co-Pi) catalyst. This remarkable feat draws inspiration from the oxygen-evolving complex (OEC) found within Photosystem II (PSII) of natural photosynthesis [169]. The newly developed Co-Pi catalyst effectively captures the key elements and functionalities of this biological marvel, paving the way for advancements in artificial photosynthesis technologies. When a widely available metal (cobalt) is oxidized in phosphate-buffered solutions at neutral pH, the Co-Pi catalyst self-assembles similarly to the OEC in PSII. In both freshwater and seawater at room temperature, this Co-Pi catalyst exhibits high activity. It is a promising catalyst for water splitting since it activates water by proton-coupled electron transfer and has self-healing qualities. A novel method for fabricating $Co_3O_4/TiO_2/Si$ nanorod (NR) catalysts was presented by Tang et al. [170], utilizing metal-organic frameworks (MOFs) as templates. The inherent advantages of MOFs, including their large specific surface area and porous channel structure, were leveraged in this approach to simultaneously enhance the optical response of Co_3O_4 and augment surface water oxidation kinetics. The resulting photoanode, derived from MOFs and composed of $Co_3O_4/TiO_2/Si$ NR, exhibited a synergistic effect arising from the combination of Co_3O_4, titanium dioxide (TiO_2), and silicon nanorods (Si NR). This synergism manifested as a significant increase in photocurrent density and photoconversion efficiency when utilized in alkaline electrolytes. Consequently, the photoanode facilitated more effective water splitting for solar energy conversion.

A recent study by Prabu et al. [1721] meticulously investigated the impact of nickel (Ni) doping on the performance of NixMo$_{1-x}$/ZIF-67@SiO$_2$ yolk-shell catalysts for formic acid dehydrogenation. A gradual enhancement in catalytic performance was observed with increasing Ni content. Among the assessed catalysts, the Ni$_{0.8}$Mo$_{0.2}$/ZIF-67@SiO$_2$ yolk-shell exhibited the most exceptional catalytic efficiency. It demonstrated a remarkable turnover frequency (TOF) of approximately 183 h^{-1} at 25 °C, indicative of a rapid catalytic reaction with complete conversion of formic acid. This catalyst further manifested a hydrogen selectivity of nearly 100 %, with no measurable CO production, ensuring the generation of clean hydrogen. Even after undergoing 10 reaction cycles, an impressive 99 % of its initial activity was retained, highlighting its long-term stability and durability. Understanding the impact of Ni doping on NixMo$_{1-x}$/ZIF-67@SiO$_2$ catalysts for formic acid dehydrogenation holds significant scientific value. By optimizing the Ni content and exploiting the synergistic effects, researchers can develop highly efficient and robust catalysts for this clean and sustainable hydrogen production pathway.

Ball et al. [172] leveraged the computational power of density functional theory (DFT) calculations to meticulously predict the catalytic activity of a specific triazine framework named SiPF-Bpy-CTF for the hydrogen evolution reaction (HER). As depicted in Fig. 12, the presented study commenced with a meticulous investigation into the electronic properties of pristine Bpy-CTF. A band gap of 1.93 eV is demonstrated by this material, thereby prompting additional scientific inquiry. To scrutinize the possibility of reducing the band gap, a meticulous strategy involving co-doping and substitution was applied to the Bpy-CTF framework. The implementation of this multifaceted approach encompassed the co-doping of Bpy-CTF with Si and P atoms, succeeded by the deliberate substitution of hydrogen atoms located on the bipyridine (Bpy) ligands at the P-site with F atoms. This systematic modification warrants a closer scientific examination to illuminate its impact on the electronic properties of Bpy-CTF. This manipulation

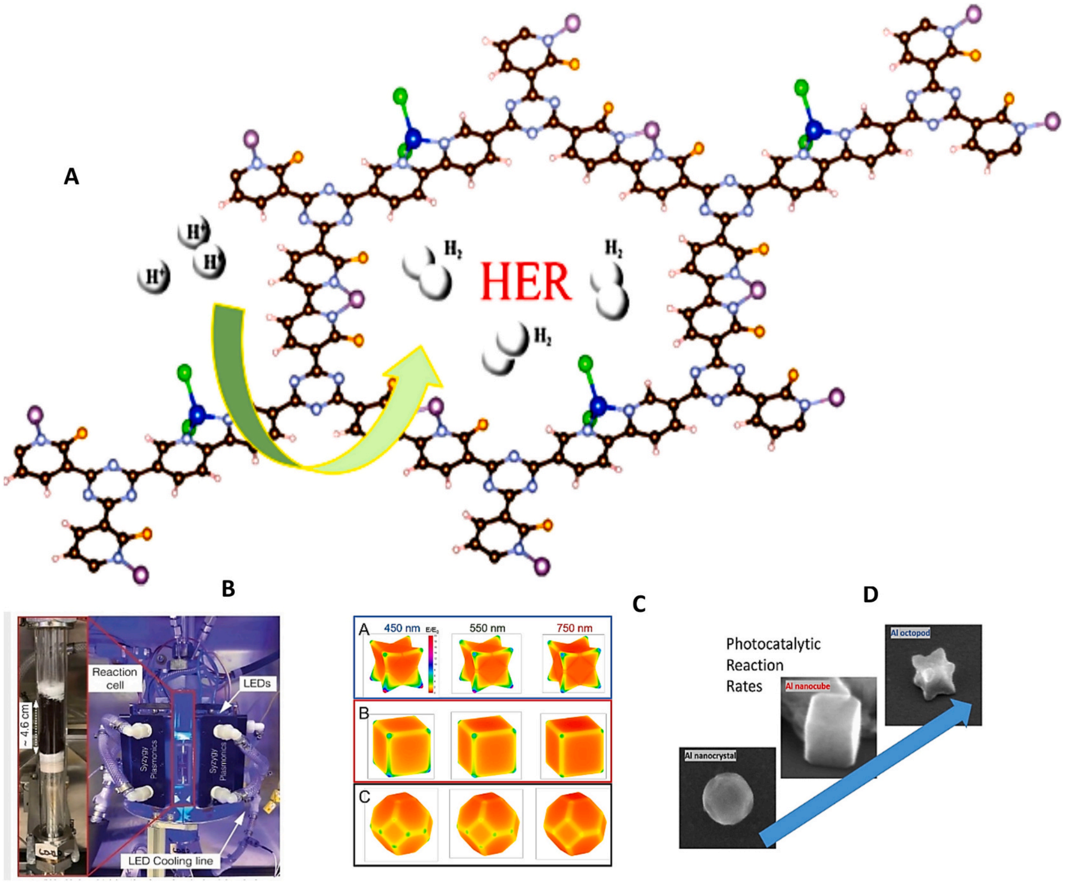

Fig. 12. Triazine framework (SiPF-BpyCTF) for the hydrogen evolution reaction (HER). B. A reaction cell used on tests of copper-iron plasmonic photocatalysts for hydrogen production from ammonia at Syzygy Plasmonics in Houston [173]. C. Different shape of the plasmonic nanoparticle D. Shape-dependent activity of the plasmonic nanoparticle [174].

successfully engineered the SiPF-Bpy-CTF triazine framework, exhibiting a remarkably narrow band gap of merely 7 eV. The present study, through meticulous energetic analysis, identified both the nitrogen atoms within the triazine moiety and the Si-site as advantageous adsorption sites for atomic hydrogen. Predicting the HER activity of SiPF-Bpy-CTF through DFT calculations represents a significant step forward in identifying promising materials for sustainable hydrogen production. By guiding further experimental studies and material optimization, this computational approach can accelerate the development of efficient and cost-effective HER catalysts, contributing to the realization of a clean and sustainable energy future. To validate the results and confirm the actual catalytic performance of SiPF-Bpy-CTF, experimental investigations are still required. Experimental studies may provide crucial evidence and insights into the actual catalytic activity and suitability of SiPF-Bpy-CTF for the hydrogen evolution reaction.

The study by Railey et al. [175] focused on the Si@ZIF-8 core-shell structure for electrochemical hydrogen production. The Si@ZIF-8 refers to silicon nanoparticles (NPs) encapsulated within a ZIF-8 (zeolitic imidazolate framework-8) shell. This core-shell structure offers several advantages for hydrogen production. According to the study, the Si@ZIF-8 electrode exhibited a high capacity of 830 $\mathrm{mAhg^{-1}}$ when operated at a current density of 200 milliamps per gram (200 $\mathrm{mAg^{-1}}$). This high capacity is attributed to the presence of uniformly distributed silicon nanoparticles within the carbon matrix. The silicon nanoparticles play a crucial role in facilitating efficient electrochemical hydrogen production. One notable aspect highlighted in the study is the remarkable stability of the Si@C electrode over extended cycling. The carbon coating surrounding the silicon nanoparticles is considered responsible for this stability. The soft nature of the carbon coating helps to mitigate the large volumetric changes that occur during the alloying and dealloying processes of silicon. This mitigation of volumetric changes contributes to the electrode's stability. The uniformly distributed silicon nanoparticles within the carbon matrix, along with the protective carbon coating, contributed to the high stability of the electrode.

Very recently, researchers have investigated the integration of non-noble metal nanoparticles with semiconductor materials to enhance plasmonic effects specifically for hydrogen production. The integration of non-noble metal nanoparticles with semiconductor materials for enhanced plasmonic effects is an exciting development in the field. The generation of hot carriers by plasmonic particles and their utilization in driving chemical reactions through hybrid antenna reactors shows immense promise for unlocking more efficient hydrogen production. The study by Yuan et al. [173], where gram-scale quantities of hydrogen gas were produced from ammonia using copper-iron nanoparticles under LED illumination (Fig. 12B), highlights the comparable efficiencies and reactivities of these particles with copper-ruthenium. This demonstrates that non-noble metal nanoparticles can exhibit similar performance to noble metals in plasmonic photocatalysis. The research by Yuan et al. [173] emphasized the significance of nanoparticle morphology in plasmonic photocatalysis. It has been scientifically established that the geometry of plasmonic nanoparticles critically influences their efficacy. Each distinct shape fosters unique plasmonic characteristics, leading to enhanced light absorption and scattering. This phenomenon can be attributed to the interaction of light with the localized surface plasmons, and collective oscillations of the conduction electrons induced by the incident light. The specific shape dictates the resonance frequency, intensity, and spatial distribution of these plasmons, ultimately determining the overall light-matter interaction

(Fig. 12C-D). The study revealed that nanocrystals with more cuspate shapes exhibited greater reactivity rates and lower activation barriers, resulting in improved efficiency for hot electron-driven reactions. These findings further emphasize the importance of optimizing the shape and morphology of plasmonic materials for efficient photocatalytic hydrogen production. By tailoring the morphology to specifically enhance reaction rates and reduce activation barriers, researchers can improve the overall performance and energy conversion efficiency of plasmonic photocatalytic systems. The integration of plasmonic materials with semiconductor photocatalysts, the generation of hot carriers, and the optimization of nanoparticle morphology all contribute to enhancing the efficiency of photocatalytic hydrogen production. These advancements may provide promising avenues for developing more efficient and sustainable methods of hydrogen generation, which is crucial for photocatalytic hydrogen production.

Biosilicification is indeed the process of polymerizing biologically available monomeric silicic acid into insoluble silica in various organisms such as protists, diatoms, sponges, mollusks, and higher plants. The ability to create silica-based nanostructures encapsulating biomolecules opens possibilities for H_2 production through photocatalysis [175]. The cellular and metabolic processes related to biosilicification are regulated by silicon transporters that facilitate the uptake of silicic acid from the surrounding aqueous environment. Silicic acid is then transformed and condensed into amorphous silica within membrane-bound deposition vesicles. This transformation is mediated by a variety of proteins [176]. These proteins play a crucial role in the formation and deposition of silica structures. It is worth noting that similar mechanisms may govern biosilicification in other organisms that engage in silicification. While the specific proteins and processes involved may vary, the general principles of cellular intake, transformation, and deposition of silicic acid are likely to be present. Recent studies have shown that proteins from diverse functional groups can interact with silica, leading to the formation of protein/silica composite shells. This opens up possibilities for unlimited functionalization of silica-based materials, including the integration of optical elements with specific waveguide properties for photocatalysis applications [177].

It is worth noting that the incorporation of silicon into MOFs is a relatively recent area of research, and the development of silicon-based MOFs is still in its early stages. However, the unique properties of silicon, combined with the tunability and porosity of MOFs, offer exciting opportunities for the design of new materials with enhanced functionalities. Continued research in this field may lead to the discovery of novel silicon-based MOFs and expand their potential in silicon-based catalysts and accelerate the transition to a hydrogen-based economy.

Silicon, as a key element in catalytic applications, when integrated into MOFs, can introduce additional functionalities that are critical for electrocatalysis and photocatalysis. The use of silicon-containing ligands, such as organosilanes or organosilicates, in MOF synthesis allows for the creation of structures that benefit from both the tunability of MOFs and the advantageous properties of silicon. These silicon-based MOFs have been shown to improve electrocatalytic performance by mass facilitating effective transport and enhancing access to active sites, which are essential for water splitting reactions. The fabrication of nanostructured catalysts, such as Co3O4/TiO2/Si nanorods, using MOFs as templates, has further highlighted the synergy between silicon and other components in optimizing the optical response and enhancing reaction kinetics for solar energy conversion. While silicon-based MOFs are still in the early stages of research, their potential to drive advancements in renewable energy production is significant. The exploration of such materials could lead to breakthroughs in photocatalysis.

5. Conclusion and perspectives

Silicon nanosheets, nanowires, silicon carbide, heterojunctions, and metal-organic framework (MOF) silicon catalysts are among the various silicon-based materials that have been investigated for their potential in hydrogen production through photocatalysis. When comparing these silicon-based catalysts for hydrogen production, various factors should be considered, including their catalytic activity, stability, cost-effectiveness, and scalability. The specific performance of each catalyst type can vary depending on the synthesis method, surface modifications, catalyst loading, and reaction conditions. Controlling the purity of the synthesized materials is therefore important to ensure high conversion efficiencies. Several key factors contributed to the impressive hydrogen generation (4437 μmol h^{-1} g^{-1}) of Si achieved by these silicon nanoparticles. It is important to note that this achievement represents the highest reported value thus far, demonstrating the potential of silicon nanoparticles as highly efficient catalysts for hydrogen production. To achieve optimally performing Si-photocatalysts, it is indeed important to balance the factors of crystallinity, oxidation, and particle sintering. Although maximizing crystallinity in silicon nanoparticles undoubtedly enhances their catalytic activity for hydrogen evolution, other significant factors play equally crucial roles. Minimizing oxidation and reducing grain boundaries resulting from particle sintering are equally vital aspects for achieving optimal performance. To address this issue, it is recommended to take care in storing the Si nanoparticles (NPs) to minimize oxidation. This could involve storing them in a controlled environment, such as in an inert gas atmosphere or a vacuum, to prevent exposure to oxygen and moisture, which are the primary causes of oxidation. Developing approaches for surface protection becomes crucial to enhance the longevity of Si nanoparticles (Si NPs) utilized in photocatalytic experiments. These approaches could involve the use of protective coatings or surface modifications to create a barrier between the NPs and the surrounding environment, thereby reducing oxidation and enhancing the stability of the NPs over time. By incorporating optimal heterojunctions and employing surface protection mechanisms such as Si/polymer hybrids, the stability, charge carrier separation, and overall performance of photocatalysts can be enhanced. However, implementing all-solid-state heterojunctions or *Z*-scheme systems can be technically challenging and requires the development of suitable materials and device architectures. To further increase the effectiveness of solar-to-fuel transformation, techniques such as plasmon composites can be employed. Plasmon composites can expand the optical absorption range into the visible spectrum, thereby increasing the efficiency of light absorption by silicon. Laser ablation is one approach that offers precise control over the fabrication process. However, it requires sophisticated equipment and can be costly to implement on a large scale. Some approaches, such as the use of co-catalysts or sacrificial agents, can enhance hydrogen generation performance. However, they may also increase costs and raise environmental concerns. Balancing the performance benefits with economic and environmental considerations is a key challenge in the development of these systems. Developing a synthesis method that is simple, economically feasible, and environmentally friendly is crucial for the widespread implementation of silicon-based heterojunctions for sustainable hydrogen production.

CRediT authorship contribution statement

Aminul Islam: Writing – review & editing, Writing – original draft, Supervision, Resources, Investigation, Data curation, Funding acquisition, Conceptualization. **Md. Tarekul Islam:** Writing – original draft, Software, Resources, Investigation. **Siow Hwa Teo:** Writing – original draft, Software, Resources, Formal analysis, Data curation. **Hasan Mahmud:** Writing – original draft, Validation, Resources, Investigation. **A.M. Swaraz:** Writing – original draft, Validation, Resources, Conceptualization. **Ariyan Islam Rehan:** Writing – original draft, Software, Formal analysis, Data curation. **Adiba Islam Rasee:** Writing – original draft, Software, Resources, Data curation. **Khadiza Tul Kubra:** Writing – original draft, Visualization, Methodology, Investigation, Data curation. **Md. Munjur Hasan:** Writing – original draft, Validation, Resources, Investigation. **Md. Shad Salman:** Writing – original draft, Visualization, Validation, Resources. **R.M. Waliullah:** Writing –

original draft, Resources, Investigation, Formal analysis, Data curation. **Md. Nazmul Hasan:** Writing – original draft, Resources, Investigation, Formal analysis, Conceptualization. **Md. Chanmiya Sheikh:** Writing – original draft, Validation, Resources, Conceptualization. **Tetsuya Uchida:** Validation, Resources, Conceptualization. **Mrs Eti Awual:** Writing – original draft, Validation, Methodology, Conceptualization. **Mohammed Sohrab Hossain:** Validation, Resources, Investigation, Data curation. **Hussein Znad:** Resources, Methodology, Formal analysis. **Md. Rabiul Awual:** Writing – review & editing, Writing – original draft, Project administration, Funding acquisition, Conceptualization.

Declaration of competing interest

The authors declare that they have no known competing financial interests or personal relationships that could have appeared to influence the work reported in this paper.

Acknowledgments

This research was supported by the Bangladesh Energy and Power Research Council (BEPRC) and carried out at the Hydrogen Energy and CO₂ Conversion Laboratory, Department of Petroleum and Mining Engineering, Jashore University of Science and Technology, Jashore 7408, Bangladesh.

Data availability

The data that has been used is confidential.

References

[1] Pijpers JJ, Winkler MT, Surendranath Y, Buonassisi T, Nocera DG. Light-induced water oxidation at silicon electrodes functionalized with a cobalt oxygen-evolving catalyst. Proc Natl Acad Sci 2011;108(25):10056–61.
[2] Poonia K, Nguyen TTH, Singh P, Ahamad T, Thakur S, Nguyen VH, et al. Ni-based plasmonic photocatalysts for solar to energy conversion: a review. Mol Catal 2024;561:114166.
[3] Mareev E, Pushkin A, Migal E, Lvov K, Stremoukhov S, Potemkin F. Single-shot femtosecond bulk micromachining of silicon with mid-IR tightly focused beams. Sci Rep 2022;12(1):7517.
[4] Nassah Y, Benmakhlouf A, Hadjeris L, Helaimia T, Khenata R, Bouhemadou A, et al. Electronic band structure, mechanical and optical characteristics of new lead-free halide perovskites for solar cell applications based on DFT computation. Bull Mater Sci 2023;46(2):55.
[5] Soni V, Malhotra M, Singh P, Khan AAP, Bawazir WA, Nguyen VH, et al. Recent updates on full solar spectrum metal sulphides photocatalyst for hydrogen peroxide generation: modification strategies and mechanistic insights. Journal of environmental. Chem Eng 2024:115151.
[6] Teitsworth TS, Hill DJ, Litvin SR, Ritchie ET, Park JS, Custer Jr JP, et al. Water splitting with silicon p–i–n superlattices suspended in solution. Nature 2023;614 (7947):270–4.
[7] Malhotra M, Soni V, Kumar R, Singh P, Thakur S, Van Le Q, et al. Mofs-based S-scheme heterojunction photocatalysts: challenges and prospects to break the selectivity limitation for intensified C1 products in CO2 photoreduction. Chem Eng J 2025:160238.
[8] Poonia K, Soni V, Singh P, Chaudhary V, Thakur S, Nguyen VH, et al. Metal-free defects in 2D Nanocarbons toward photocatalytic processes: revolutionizing solar-to-energy conversion. Appl Energy 2025;382:125195.
[9] Usman M, Kavitha S, Kannah Y, Yogalakshmi KN, Sivashanmugam P, Bhatnagar A, et al. A critical review on limitations and enhancement strategies associated with biohydrogen production. Int J Hydrog Energy 2021;46(31): 16565–90.
[10] Budhraja N, Pal A, Mishra RS. Various treatment methods for enhanced bio-hydrogen production. Mater Today Proc 2023:1–6.
[11] Muduli RC, Kale P. Silicon nanostructures for solid-state hydrogen storage: A review. Int J Hydrog Energy 2023;48(4):1401–39.
[12] Li N, Xiang F, Fratalocchi A. Silicon-based Photocatalysis for green chemical fuels and carbon negative technologies. Adv Sustain Syst 2021;5(3):2000242.
[13] Chen S, Liu T, Zheng Z, Ishaq M, Liang G, Fan P, et al. Recent progress and perspectives on Sb2Se3-based photocathodes for solar hydrogen production via photoelectrochemical water splitting. J Energy Chem 2022;67:508–23.
[14] Jian J, Sun J. A review of recent progress on silicon carbide for photoelectrochemical water splitting. Sol RRL 2020;4(7):2000111.
[15] Naushad M, Kumar A, Sharma S. Graphitic carbon nitride based photocatalytic Systems for High Performance Hydrogen Production: A review. Mater Res Found 2021;100.
[16] Vinoth S, Devi KS, Pandikumar A. A comprehensive review on graphitic carbon nitride based electrochemical and biosensors for environmental and healthcare applications. TrAC Trends Anal Chem 2021;140:116274.
[17] Wudil YS, et al. Tuning of graphitic carbon nitride (g-C3N4) for Photocatalysis: A critical review. Arab J Chem 2023:104542.
[18] Reza MS, Ahmad NBH, Afroze S, Taweekun J, Sharifpur M, Azad AK. Hydrogen production from water splitting through photocatalytic activity of carbon-based materials. Chem Eng Technol 2023;46(3):420–34.
[19] Mehta A, Mishra A, Basu S, Shetti NP, Reddy KR, Saleh TA, et al. Band gap tuning and surface modification of carbon dots for sustainable environmental remediation and photocatalytic hydrogen production–A review. J Environ Manag 2019;250:109486.
[20] Chai JH, Wong BT, Juodkazis S. Black-silicon-assisted photovoltaic cells for better conversion efficiencies: a review on recent research and development efforts. Mater Today Energy 2020;18:100539.
[21] Fan Z, Cui D, Zhang Z, Zhao Z, Chen H, Fan Y, et al. Recent progress of black silicon: from fabrications to applications. Nanomaterials 2020;11(1):41.
[22] Mohsin M, Ishaq T, Bhatti IA, Jilani A, Melaibari AA, Abu-Hamdeh NH. Semiconductor nanomaterial Photocatalysts for water-splitting hydrogen production: the holy grail of converting solar energy to fuel. Nanomaterials 2023; 13(3):546.
[23] Hoti P, Das A, Maiti DK. A short review on generation of green fuel hydrogen through water splitting. Int J Hydrog Energy 2023;48(2):523–41.
[24] Ahmed I, Shi L, Pasanen H, Vivo P, Maity P, Hatamvand M, et al. There is plenty of room at the top: generation of hot charge carriers and their applications in perovskite and other semiconductor-based optoelectronic devices. Light Sci Appl 2021;10(1):174.
[25] Liu D, Li L, Gao Y, Wang C, Jiang J, Xiong Y. The nature of photocatalytic "water splitting" on silicon nanowires. Angew Chem Int Ed 2015;54(10):2980–5.
[26] Wang B, Wang Y, Lei Y, Wu N, Gou Y, Han C, et al. Mesoporous silicon carbide nanofibers with in situ embedded carbon for co-catalyst free photocatalytic hydrogen production. Nano Res 2016;9:886–98.
[27] Huang L, Huang X, Yan J, Liu Y, Jiang H, Zhang H, et al. Research progresses on the application of perovskite in adsorption and photocatalytic removal of water pollutants. J Hazard Mater 2023;442:130024.
[28] Maeng SH, Lee H, Park MS, Park S, Jeong J, Kim S. Ultrafast carbothermal reduction of silica to silicon using a CO2 laser beam. Sci Rep 2020;10(1):21730.
[29] Entwistle J, Rennie A, Patwardhan S. A review of magnesiothermic reduction of silica to porous silicon for lithium-ion battery applications and beyond. J Mater Chem A 2018;6(38):18344–56.
[30] Dong Y, Slade T, Stolt MJ, Li L, Girard SN, Mai L, et al. Low-temperature molten-salt production of silicon nanowires by the electrochemical reduction of CaSiO3. Angew Chem 2017;129(46):14645–9.
[31] Chen Z, Zhang H, Ma W, Wu J. High efficient and clean utilization of coal for the carbothermic reduction of silica. Sustain Energy Technol Assess 2022;53:102602.
[32] Liu X, Gao Y, Jin R, Luo H, Peng P, Liu Y. Scalable synthesis of Si nanostructures by low-temperature magnesiothermic reduction of silica for application in lithium ion batteries. Nano Energy 2014;4:31–8.
[33] Cordova S, Shafirovich E. Combustion synthesis of nanocrystalline silicon from silica and magnesium silicide. Mater Chem Phys 2020;254:123288.
[34] Lawrence K, Morgan S, Schaller D, Wilczak T. Environmental, health, safety, and regulatory review of selected photovoltaic options: copper sulfide/cadmium sulfide and polycrystalline silicon (No. SERI/TR-743-799). Golden, CO (United States): Solar Energy Research Inst (SERI); 1981.
[35] Hansen KC, Yaws CL. Silicon tetrafluoride generation [Patent application; from hexafluorosilicic acid]. 1982 (No. PATENTS-US-A345458).
[36] Binetti S, Libal J, Acciarri M, Di Sabatino M, Nordmark H, Øvrelid EJ, et al. Study of defects and impurities in multicrystalline silicon grown from metallurgical silicon feedstock. Mater Sci Eng B 2009;159:274–7.
[37] Erogbogbo F, Lin T, Tucciarone PM, LaJoie KM, Lai L, Patki GD, et al. On-demand hydrogen generation using nanosilicon: splitting water without light, heat, or electricity. Nano Lett 2013;13(2):451–6.
[38] Lv P, Xu C, Peng B. Design of a silicon photocatalyst for high-efficiency photocatalytic water splitting. ACS omega 2020;5(12):6358–65.
[39] Su Y, Wang C, Hong Z, Sun W. Thermal disproportionation for the synthesis of silicon nanocrystals and their photoluminescent properties. Front Chem 2021; 575.
[40] Wang J, Wang XF, Li Q, Hryciw A, Meldrum A. The microstructure of Silo thin films: from nanoclusters to nanocrystals. Philos Mag 2007;87(1):11–27.
[41] Colinge JP. Silicon-on-insulator technology: Materials to VLSI. Springer Science & Business Media; 2004.
[42] Nesbit LA. Annealing characteristics of Si-rich SiO2 films. Appl Phys Lett 1985;46 (1):38–40.
[43] Dai F, Zai J, Yi R, Gordin ML, Sohn H, Chen S, et al. Bottom-up synthesis of high surface area mesoporous crystalline silicon and evaluation of its hydrogen evolution performance. Nat Commun 2014;5(1):3605.
[44] Nakamura J, Asano N, Hieda T, Okamoto C, Katayama H, Nakamura K. Development of heterojunction back contact Si solar cells. IEEE J Photovol 2014; 4(6):1491–5.
[45] Joo BS, Kim IS, Han IK, Ko H, Kang JG, Kang G. Plasmonic silicon nanowires for enhanced heat localization and interfacial solar steam generation. Appl Surf Sci 2022;583:152563.
[46] Yang D, Mannan A, Murakami F, Tonouchi M. Rapid, noncontact, sensitive, and semiquantitative characterization of buffered hydrogen-fluoride-treated silicon wafer surfaces by terahertz emission spectroscopy. Light Sci Appl 2022;11(1): 334.

[47] Wang K, Martinsen T, Liu G, Tayyib M, Cui D, De Boer MJ, et al. Ultralow broadband reflectivity in black silicon via synergy between hierarchical texture and specific-size au nanoparticles. Adv Opt Mater 2020;8:202000668.

[48] Liu Z, Liu H, Wang X, Yang H, Gao J. Large area and broadband ultra-black absorber using microstructured aluminum doped silicon films. Sci Rep 2017;7(1):1–8.

[49] Sun Z, Chen X, He Y, Li J, Wang J, Yan H, et al. Toward efficiency limits of crystalline silicon solar cells: recent progress in high-efficiency silicon heterojunction solar cells. Adv Energy Mater 2022;12(23):2200015.

[50] Zhang Z, Martinsen T, Liu G, Tayyib M, Cui D, de Boer MJ, et al. Ultralow broadband reflectivity in black silicon via synergy between hierarchical texture and specific-size au nanoparticles. Adv Opt Mater 2020;8(19):2000668.

[51] Garin M, Heinonen J, Werner L, Pasanen TP, Vähänissi V, Haarahiltunen A, et al. Black-silicon ultraviolet photodiodes achieve external quantum efficiency above 130%. Phys Rev Lett 2020;125(11):117702.

[52] Kecebas MA, Pirouzfam N, Sendur K. Origins of the enhanced broadband absorption in black silicon. J Appl Phys 2021;129(16):163103 [3D].

[53] Marthi SR, Sekhri S, Ravindra NM. Optical properties of black silicon: an analysis. Jom 2015;67:2154–9 [Line graph].

[54] Ao X, Tong X, Sik Kim D, Zhang L, Knez M, Müller F, et al. Black silicon with controllable macropore array for enhanced photoelectrochemical performance. Appl Phys Lett 2012;101(11):111901.

[55] Meng Y, An L, Han X, Li Y, Hou C, Zhang Q, et al. Controllable (Ga1− xZnx)(N1−xOx) nanorods grown on black silicon as anodes for water splitting. Appl Surf Sci 2020;502:144174.

[56] Fan S, AlOtaibi B, Woo SY, Wang Y, Botton GA, Mi Z. High efficiency solar-to-hydrogen conversion on a monolithically integrated InGaN/GaN/Si adaptive tunnel junction photocathode. Nano Lett 2015;15(4):2721–6.

[57] Kan M, Qian X, Zhang T, Yue D, Zhao Y. Highly active IrO x nanoparticles/black Si electrode for efficient water splitting with conformal TiO2 interface engineering. ACS Sustain Chem Eng 2017;5(11):10940–6.

[58] Hossen M, Ismail ABM. Investigation on Fe2O3/por-Si photocatalyst for low-bias water-splitting. J Mater Sci Mater Electron 2018;29(18):15480–5.

[59] Okamoto H, Sugiyama Y, Nakano H. Synthesis and modification of silicon nanosheets and other silicon nanomaterials. Chemistry–A. Eur J Dermatol 2011;17(36):9864–87.

[60] Nakano H, Ikuno T. Soft chemical synthesis of silicon nanosheets and their applications. Appl Phys Rev 2016;3(4):040803.

[61] Ryu J, Jang YJ, Choi S, Kang HJ, Park H, Lee JS, et al. All-in-one synthesis of mesoporous silicon nanosheets from natural clay and their applicability to hydrogen evolution. NPG Asia Mater 2016;8(3):e248.

[62] Hwang GC, Blom DA, Vogt T, Lee J, Choi HJ, Shao S, et al. Pressure-driven phase transitions and reduction of dimensionality in 2D silicon nanosheets. Nat Commun 2018;9(1):1–9.

[63] Li S, Wang H, Li D, Zhang X, Wang Y, Xie J, et al. Siloxanes nanosheets: a metal-free semiconductor for water splitting. J Mater Chem A 2016;4(41):15841–4.

[64] Wang B, Yao L, Xu G, Zhang X, Wang D, Shu X, et al. Highly efficient photoelectrochemical synthesis of ammonia using plasmon-enhanced black silicon under ambient conditions. ACS Appl Mater Interfaces 2020;12(18):20376–82.

[65] Lu Z, Zhu J, Sim D, Zhou W, Shi W, Hng HH, et al. Synthesis of ultrathin silicon nanosheets by using graphene oxide as template. Chem Mater 2011;23(24):5293–5.

[66] Ma L, Song X, Yu Y, Chen Y. Two-dimensional Silicene/silicon Nanosheets: An emerging silicon-composed nanostructure in biomedicine. Adv Mater 2021;33(31):2008226.

[67] Islam A, Hwa Teo S, Awual MR, Taufiq-Yap YH. Ultrathin assembles of porous array for enhanced H2 evolution. Sci Rep 2020;10(1):2324.

[68] Liu Y, Xue Y, Yu H, Hui L, Huang B, Li Y. Graphdiyne ultrathin nanosheets for efficient water splitting. Adv Funct Mater 2021;31(16):2010112.

[69] Zhou L, Wang Y, Xu X, Lei W, Huang J, Chen L, et al. One-step controllable synthesis of amino-modification siloxene for enhanced solar water-splitting. J Colloid Interface Sci 2020;579:205–11.

[70] Li S, Zhang P, Song X, Gao L. Photoelectrochemical hydrogen production of TiO2 passivated Pt/Si-nanowire composite photocathode. ACS Appl Mater Interfaces 2015;7(33):18560–5.

[71] He WW, Wu KJ, Wang K, Shi TF, Wu L, Li SX, et al. Towards stable silicon nanoarray hybrid solar cells. Sci Rep 2014;4(1):3715.

[72] Oh I, Kye J, Hwang S. Enhanced photoelectrochemical hydrogen production from silicon nanowire array photocathode. Nano Lett 2012;12(1):298–302.

[73] Zang GL, Sheng GP, Shi C, Wang YK, Li WW, Yu HQ. A bio-photoelectrochemical cell with a MoS 3-modified silicon nanowire photocathode for hydrogen and electricity production. Energy Environ Sci 2014;7(9):3033–9.

[74] Yang Y, Wang M, Zhang P, Wang W, Han H, Sun L. Evident enhancement of photoelectrochemical hydrogen production by electroless deposition of MB (M= Ni, co) catalysts on silicon nanowire arrays. ACS Appl Mater Interfaces 2016;8(44):30143–51.

[75] Tran PD, Pramana SS, Kale VS, Nguyen M, Chiam SY, Batabyal SK, et al. Novel assembly of an MoS2 electrocatalyst onto a silicon nanowire array electrode to construct a photocathode composed of elements abundant on the earth for hydrogen generation. Chemistry 2012;18(44):13994–9.

[76] Zhu L, Cai Q, Liao F, Sheng M, Wu B, Shao M. Ru-modified silicon nanowires as electrocatalysts for hydrogen evolution reaction. Electrochem Commun 2015;52:29–33.

[77] Gnanasekar P, Periyanagounder D, Varadhan P, He JH, Kulandaivel J. Highly efficient and stable photoelectrochemical hydrogen evolution with 2D-NbS2/Si nanowire heterojunction. ACS Appl Mater Interfaces 2019;11(47):44179–85.

[78] Zhang L, Liu C, Wong AB, Resasco J, Yang P. MoS 2-wrapped silicon nanowires for photoelectrochemical water reduction. Nano Res 2015;8:281–7.

[79] Jiang B, Tang Z, Liao F, Lin H, Lu S, Li Y, et al. Powerful synergy: efficient Pt–au–Si nanocomposites as state-of-the-art catalysts for electrochemical hydrogen evolution. J Mater Chem A 2017;5(41):21903–8.

[80] Shen W, Ge L, Sun Y, Liao F, Xu L, Dang Q, et al. Rhodium nanoparticles/F-doped graphene composites as multifunctional electrocatalyst superior to Pt/C for hydrogen evolution and formic acid oxidation reaction. ACS Appl Mater Interfaces 2018;10(39):33153–61.

[81] Ensafi AA, Ghadirian F, Jafari-Asl M, Rezaei B. WS 2 grafted on silicon and nano-silicon particles etched: a high-performance electrocatalyst for hydrogen evolution reaction. J Iran Chem Soc 2018;15:613–20.

[82] Dang Q, Liao F, Sun Y, Zhang S, Huang H, Shen W, et al. Rhodium/silicon quantum dot/carbon quantum dot composites as highly efficient electrocatalysts for hydrogen evolution reaction with Pt-like performance. Electrochim Acta 2019;299:828–34.

[83] Chiani E, Azizi SN, Ghasemi S. PdCu bimetallic nanoparticles decorated on ordered mesoporous silica (SBA-15)/MWCNTs as superior electrocatalyst for hydrogen evolution reaction. Int J Hydrog Energy 2021;46(50):25468–85.

[84] Ensafi AA, Jafari-Asl M, Rezaei B. Graphene/nano-porous silicon and graphene/bimetallic silicon nanostructures (Pt–M, M: Pd, Ru, Rh), efficient electrocatalysts for the hydrogen evolution reaction. Phys Chem Chem Phys 2015;17(37):23770–82.

[85] Perez Bakovic SI, Acharya P, Greenlee LF. Electrochemical activation of silicon: enhancing hydrogen production from FeNi Electrocatalysts. Energy Fuel 2022;36(13):7158–65.

[86] Gao J, Sahli F, Liu C, Ren D, Guo X, Werner J, et al. Solar water splitting with perovskite/silicon tandem cell and TiC-supported Pt nanocluster electrocatalyst. Joule 2019;3(12):2930–41.

[87] He Y, Wang TL, Zhang M, Wang TW, Wu LF, Zeng L, et al. Discovery and facile synthesis of a new silicon based family as efficient hydrogen evolution reaction catalysts: a computational and experimental investigation of metal monosilicides. Small 2021;17(8):2006153.

[88] Vinodh R, Deviprasath C, Gopi CVM, Kummara VGR, Atchudan R, Ahamad T, et al. Novel 13X zeolite/PANI electrocatalyst for hydrogen and oxygen evolution reaction. Int J Hydrog Energy 2020;45(53):28337–49.

[89] Lu Y, Wei Z, Salke NP, Yu L, Yan H. Enhanced electron transport in rutile TiO2 nanowires via H2S-assisted incorporation of dissolved silicon for solar-driven water splitting. Appl Catal B Environ 2019;244:767–72.

[90] Nguyen TL, Pham TH, Myung Y, Jung SH, Tran MH, Mapari MG, et al. Enhanced photocatalytic activity in water splitting for hydrogen generation by using TiO2 coated carbon fiber with high reusability. Int J Hydrog Energy 2022;47(98):41621–30.

[91] Ng KH, Yuan LS, Cheng CK, Chen K, Fang C. TiO2 and ZnO photocatalytic treatment of palm oil mill effluent (POME) and feasibility of renewable energy generation: A short review. J Clean Prod 2019;233:209–25.

[92] Liu L, Cao Y, He J, Qi X, Shi W, Yang Q. Solution fabrication of large-area Si/TiO2 Core/Shell nanowire arrays modified by au nanoparticles with high Photoactivity for solar water splitting. J Nanosci Nanotechnol 2013;13(10):6835–40.

[93] Dong Z, Ding D, Li T, Ning C. High-efficiency photoelectrochemical water splitting with heterojunction photoanode of In2O3-x nanorods/black Ti–Si–O nanotubes. Int J Hydrog Energy 2019;44(33):17611–21.

[94] Lu KQ, Lin X, Tang ZR, Xu YJ. Silicon nanowires@ Co3O4 arrays film with Z-scheme band alignment for hydrogen evolution. Catal Today 2019;335:294–9.

[95] Hwang YJ, Wu CH, Hahn C, Jeong HE, Yang P. Si/InGaN core/shell hierarchical nanowire arrays and their photoelectrochemical properties. Nano Lett 2012;12(3):1678–82.

[96] Moses PG, Van de Walle CG. Band bowing and band alignment in InGaN alloys. Appl Phys Lett 2010;96(2):021908.

[97] Chen H, Wang P, Wang X, Wang X, Rao L, Qian Y, et al. 3D InGaN nanowire arrays on oblique pyramid-textured Si (311) for light trapping and solar water splitting enhancement. Nano Energy 2021;83:105768.

[98] Hamdi A, Boussekey L, Roussel P, Addad A, Ezzaouia H, Boukherroub R, et al. Hydrothermal preparation of MoS2/TiO2/Si nanowires composite with enhanced photocatalytic performance under visible light. Mater Des 2016;109:634–43.

[99] Qiao L, Liao M, Fang K, He X, Zhang Y. Enhancement of photoelectrochemical hydrogen evolution of p-type silicon nanowires array by loading MoS2. Silicon 2019;11(4):1963–70.

[100] Sk MA, Ng MF, Huang L, Lim KH. Modulating the electronic properties of germanium nanowires via applied strain and surface passivation. Phys Chem Chem Phys 2013;15(16):5927–35.

[101] Li J, Zhao Z, Ma Y, Qu Y. Graphene and their hybrid electrocatalysts for water splitting. ChemCatChem 2017;9(9):1554–68.

[102] Zhou X, Li X, Gao Q, Yuan J, Wen J, Fang Y, et al. Metal-free carbon nanotube–SiC nanowire heterostructures with enhanced photocatalytic H 2 evolution under visible light irradiation. Cat Sci Technol 2015;5(5):2798–806.

[103] Yoo SC, Kang B, Van Trinh P, Phuong DD, Hong SH. Enhanced mechanical and wear properties of Al6061 alloy nanocomposite reinforced by CNT-template-grown core–shell CNT/SiC nanotubes. Sci Rep 2020;10(1):12896.

[104] Jian JX, Jokubavicius V, Syväjärvi M, Yakimova R, Sun J. Nanoporous cubic silicon carbide photoanodes for enhanced solar water splitting. ACS Nano 2021;15(3):5502–12.

[105] Kato M, Yasuda T, Miyake K, Ichimura M, Hatayama T. Epitaxial p-type SiC as a self-driven photocathode for water splitting. Int J Hydrog Energy 2014;39(10):4845–9.

[106] Tae Song J, Mashiko H, Kamiya M, Nakamine Y, Ohtomo A, Iwasaki T, et al. Improved visible light driven photoelectrochemical properties of 3C-SiC semiconductor with Pt nanoparticles for hydrogen generation. Appl Phys Lett 2013;103(21):213901.

[107] Jian J, Shi Y, Syväjärvi M, Yakimova R, Sun J. Cubic SiC Photoanode coupling with Ni: FeOOH oxygen-evolution cocatalyst for sustainable photoelectrochemical water oxidation. Sol RRL 2020;4(1):1900364.

[108] Gondal MA, Ilyas AM, Baig U. Facile synthesis of silicon carbide-titanium dioxide semiconducting nanocomposite using pulsed laser ablation technique and its performance in photovoltaic dye sensitized solar cell and photocatalytic water purification. Appl Surf Sci 2016;378:8–14.

[109] He C, Wu X, Shen J, Chu PK. High-efficiency electrochemical hydrogen evolution based on surface autocatalytic effect of ultrathin 3C-SiC nanocrystals. Nano Lett 2012;12(3):1545–8.

[110] Han T, Privitera S, Milazzo RG, Bongiorno C, Di Franco S, La Via F, et al. Photo-electrochemical water splitting in silicon based photocathodes enhanced by plasmonic/catalytic nanostructures. Mater Sci Eng B 2017;225:128–33.

[111] Islam MR, Islam MS, Mitul AF, Mojumder MRH, Islam AJ, Stampfl C, et al. Superior tunable photocatalytic properties for water splitting in two dimensional GeC/SiC van der Waals heterobilayers. Sci Rep 2021;11(1):17739.

[112] Liu JQ, Chung HJ, Kuhr T, Li Q, Skowronski M. Structural instability of 4H–SiC polytype induced by n-type doping. Appl Phys Lett 2002;80(12):2111–3.

[113] Bean JC. Silicon-based semiconductor heterostructures: column IV bandgap engineering. Proc IEEE 1992;80(4):571–87.

[114] Islam A, Teo SH, Awual MR, Taufiq-Yap YH. Assessment of clean H2 energy production from water using novel silicon photocatalyst. J Clean Prod 2020;244:118805.

[115] Ma J, Gao C, Low J, Liu D, Lian X, Zhang H, et al. Fundamental insights into surface modification of silicon material toward improved activity and durability in photocatalytic hydrogen production: a case study of pre-lithiation. J Phys Chem C 2021;125(10):5542–8.

[116] Ma W, Li J, Sun H, Chen J, Wang D, Mao Z. Robust hydrogen generation over layered crystalline silicon materials via integrated H2 evolution routes. Int J Hydrog Energy 2020;45(38):19007–16.

[117] Serafin J, Soler L, Vega D, Rodríguez Á, Llorca J. Macroporous silicon coated with M/TiO2 (M= au, Pt) as a highly efficient photoreactor for hydrogen production. Chem Eng J 2020;393:124701.

[118] Teo SH, Islam A, Taufiq-Yap YH, Awual MR. Introducing the novel composite photocatalysts to boost the performance of hydrogen (H2) production. J Clean Prod 2021;313:127909.

[119] Li X, Lv G, Ma W, Li S, Yang J, Zhang R, et al. Photocatalytic H2 evolution by AgNP@PSi/SiNS composite derived from diamond-wire sawing silicon waste. Sol Energy Mater Sol Cells 2022;236:111495.

[120] Islam A, Teo SH, Awual MR, Taufiq-Yap YH. Improving the hydrogen production from water over MgO promoted Ni–Si/CNTs photocatalyst. J Clean Prod 2019;238:117887.

[121] Jang YJ, Ryu J, Hong D, Park S, Lee JS. A multi-stacked hyperporous silicon flake for highly active solar hydrogen production. Chem Commun 2016;52:10221–4. https://doi.org/10.1039/C6CC04775K.

[122] Curtis IS, Wills RJ, Dasog M. Photocatalytic hydrogen generation using mesoporous silicon nanoparticles: influence of magnesiothermic reduction conditions and nanoparticle aging on the catalytic activity. Nanoscale 2021;13:2685–92. https://doi.org/10.1039/D0NR07463B.

[123] Sun H, Chen J, Liu S, Agrawal DK, Zhao Y, Wang D, et al. Photocatalytic H2 evolution of porous silicon derived from magnesiothermic reduction of mesoporous SiO2. Int J Hydrog Energy 2019;44:7216–21.

[124] Song H, Liu D, Yang J, Wang L, Xu H, Xiong Y. Highly crystalline mesoporous silicon spheres for efficient visible photocatalytic hydrogen evolution. ChemNanoMat 2017;3(1):22–6.

[125] Sugimoto H, Zhou H, Takada M, Fushimi J, Fujii M. Visible-light driven photocatalytic hydrogen generation by water-soluble all-inorganic core–shell silicon quantum dots. J Mater Chem A 2020;8:15789.

[126] Riyajuddin S, Sultana J, Siddiqui SA, Kumar S, Badhwar D, Yadav SS, et al. Silicon nanowire–ta 2 O 5–NGQD heterostructure: an efficient photocathode for photoelectrochemical hydrogen evolution. Sustain Energy Fuels 2022;6(1):197–208.

[127] Bett AJ, Winkler KM, Bivour M, Cojocaru L, Kabakli OS, Schulze PS, et al. Semi-transparent perovskite solar cells with ITO directly sputtered on Spiro-OMeTAD for tandem applications. ACS Appl Mater Interfaces 2019;11(49):45796–804.

[128] Zhang H, Zhu L, Guo L, Liu Y, Wan Q. N-type polycrystalline Si thick films deposited on SiNx-coated metallurgical grade Si substrates. J Mater Sci Technol 2015;31(1):65–9.

[129] Huang D, Li L, Wang K, Li Y, Feng K, Jiang F. Wittichenite semiconductor of Cu3BiS3 films for efficient hydrogen evolution from solar driven photoelectrochemical water splitting. Nat Commun 2021;12(1):3795.

[130] Bao XQ, Cerqueira MF, Alpuim P, Liu L. Silicon nanowire arrays coupled with cobalt phosphide spheres as low-cost photocathodes for efficient solar hydrogen evolution. Chem Commun 2015;51(53):10742–5.

[131] Yu J, He Q, Yang G, Zhou W, Shao Z, Ni M. Recent advances and prospective in ruthenium-based materials for electrochemical water splitting. ACS Catal 2019;9(11):9973–10011.

[132] Zeng Q, Chang S, Beyhaqi A, Lian S, Xu H, Xie J, et al. Efficient solar hydrogen production coupled with organics degradation by a hybrid tandem photocatalytic fuel cell using a silicon-doped TiO2 nanorod array with enhanced electronic properties. J Hazard Mater 2020;394:121425.

[133] Lin Y, Jiang Z, Zhu C, Hu X, Zhu H, Zhang X, et al. The optical absorption and hydrogen production by water splitting of (Si, Fe)-codoped anatase TiO2 photocatalyst. Int J Hydrog Energy 2013;38(13):5209–14.

[134] Su Y, Chen S, Quan X, Zhao H, Zhang Y. A silicon-doped TiO2 nan Jin otube arrays electrode with enhanced photoelectrocatalytic activity. Appl Surf Sci 2008;255(5):2167–72.

[135] Jin R, Wu Z, Liu Y, Jiang B, Wang H. Photocatalytic reduction of NO with NH3 using Si-doped TiO2 prepared by hydrothermal method. J Hazard Mater 2009;161(1):42–8.

[136] Zhang C, Chang S, Dan Y. Advances in ultrashallow doping of silicon. Adv Phys X 2021;6(1):1871407.

[137] Sun X, Jiang J, Yang Y, Shan Y, Gong L, Wang M. Enhancing the performance of Si-based photocathodes for solar hydrogen production in alkaline solution by facilely intercalating a sandwich N-doped carbon nanolayer to the interface of Si and TiO2. ACS Appl Mater Interfaces 2019;11(21):19132–40.

[138] Dong R, Han P, Arora H, Ballabio M, Karakus M, Zhang Z, et al. High-mobility band-like charge transport in a semiconducting two-dimensional metal–organic framework. Nat Mater 2018;17(11):1027–32.

[139] Zhang X, Zhang B, Zuo Z, Wang M, Shen Y. N/Si co-doped oriented single crystalline rutile TiO 2 nanorods for photoelectrochemical water splitting. J Mater Chem A 2015;3(18):10020–5.

[140] Sim U, Moon J, An J, Kang JH, Jerng SE, Moon J, et al. N-doped graphene quantum sheets on silicon nanowire photocathodes for hydrogen production. Energy Environ Sci 2015;8(4):1329–38.

[141] Wang A, Zhao L, Yu J, Zhou W, Chu B, Liu H. Co nanoparticles@ N-doped carbon coated on carbon nanotube@ defective silica as non-noble photocathode for efficient photoelectrochemical hydrogen generation. Int J Hydrog Energy 2018;43(19):9279–86.

[142] Li J, Zhu JJ. Quantum dots for fluorescent biosensing and bio-imaging applications. Analyst 2013;138(9):2506–15.

[143] Oh IKV, Molina SI, Borisevich AY, Luo W, Werner P, et al. Point defect configurations of supersaturated au atoms inside Si nanowires. Nano Lett 2008;8(4):1016–9.

[144] Zhao Y, Anderson NC, Zhu K, Aguiar JA, Seabold JA, Lagemaat JVD, et al. Oxidatively stable nanoporous silicon photocathodes with enhanced onset voltage for photoelectrochemical proton reduction. Nano Lett 2015;15(4):2517–25.

[145] Zhang H, Ding Q, He D, Liu H, Liu W, Li Z, et al. A p-Si/NiCoSe x core/shell nanopillar array photocathode for enhanced photoelectrochemical hydrogen production. Energy Environ Sci 2016;9(10):3113–9.

[146] Jin S. Photoelectrochemical solar energy conversion and Electrocatalysis using earth-abundant nanomaterials. In: Electrochemical society meeting abstracts 228. vol. 43. The Electrochemical Society, Inc.; 2015. p. 1701.

[147] Huang Z, Zhong P, Wang C, Zhang X, Zhang C. Silicon nanowires/reduced graphene oxide composites for enhanced photoelectrochemical properties. ACS Appl Mater Interfaces 2013;5(6):1961–6.

[148] Meng H, Fan K, Low J, Yu J. Electrochemically reduced graphene oxide on silicon nanowire arrays for enhanced photoelectrochemical hydrogen evolution. Dalton Trans 2016;45(35):13717–25.

[149] Kim HJ, Lee SE, Lee J, Jung JY, Lee ES, Choi JH, et al. Gold-coated silicon nanowire–graphene core–shell composite film as a polymer binder-free anode for rechargeable lithium-ion batteries. Phys E 2014;61:204–9.

[150] Xia F, Kwon S, Lee WW, Liu Z, Kim S, Song T, et al. Graphene as an interfacial layer for improving cycling performance of Si nanowires in lithium-ion batteries. Nano Lett 2015;15(10):6658–64.

[151] Xu J, Wang L, Cao X. Polymer supported graphene–CdS composite catalyst with enhanced photocatalytic hydrogen production from water splitting under visible light. Chem Eng J 2016;283:816–25.

[152] Bae H, Rho H, Min JW, Lee YT, Lee SH, Fujii K, et al. Improvement of efficiency in graphene/gallium nitride nanowire on silicon photoelectrode for overall water splitting. Appl Surf Sci 2017;422:354–8.

[153] Fellahi O, Sarma RK, Das MR, Saikia R, Marcon L, Coffinier Y, et al. The antimicrobial effect of silicon nanowires decorated with silver and copper nanoparticles. Nanotechnology 2013;24(49):495101.

[154] Yang H, Ji S, Yin J, Feng W, Kong W, Wen Z. Petal-like metal-organic framework stabilized Si@ C with long cycle life and excellent kinetics. J Colloid Interface Sci 2021;586:381–90.

[155] BoorboorAjdari F, Ostad MI, Shahrak MN, Ershadi M, Malek SS, Ghasemi F, et al. Investigating MCM-41/metal-organic framework nanocomposites as silicon-containing electrodes for supercapacitor. Surf Interfaces 2022;29:101796.

[156] Ghafari S, Naderi N, Eshraghi MJ, Kazemzad M. Temperature-dependent photonic properties of porous-shaped metal-organic frameworks on porous silicon substrates. Sensors Actuators A 2022;337:113443.

[157] Rimoldi M, Gallington LC, Chapman KW, MacRenaris K, Hupp JT, Farha OK. Catalytically active silicon oxide nanoclusters stabilized in a metal–organic framework. Chemistry 2017;23(35):8532–6.

[158] Liu Z, Stern CL, Lambert JB. Metal-organic frameworks from dipodal and tripodal silicon-centered tetrahedral ligands. Organometallics 2009;28(1):84–93.

[159] Pugh D, Ashworth E, Robertson K, Delmas LC, White AJ, Horton PN, et al. Metal–organic frameworks constructed from group 1 metals (Li, Na) and silicon-centered linkers. Cryst Growth Des 2018;19(1):487–97.

[160] Lambert JB, Liu Z, Liu C. Metal-organic frameworks from silicon-and germanium-centered tetrahedral ligands. Organometallics 2008;27(7):1464–9.

[161] Zhong S, Liu B, Xia Y, Liu J, Liu J, Shen Z, et al. The study on the properties of black multicrystalline silicon solar cell varying with the diffusion temperature. Energy Procedia 2012;14:505–11.

[162] Han Y, Qi P, Zhou J, Feng X, Li S, Fu X, et al. Metal–organic frameworks (Mofs) as sandwich coating cushion for silicon anode in lithium-ion batteries. ACS Appl Mater Interfaces 2015;7(48):26608–13.

[163] Yang D, Mei S, Wen Z, Wei X, Cui Z, Yang B, et al. Dual-emission of silicon nanoparticles encapsulated lanthanide-based metal-organic frameworks for ratiometric fluorescence detection of bacterial spores. Microchim Acta 2020;187(12):1–9.

[164] Wang CP, Liu HY, Bian G, Gao X, Zhao S, Kang Y, et al. Metal-layer assisted growth of ultralong quasi-2D MOF nanoarrays on arbitrary substrates for accelerated oxygen evolution. Small 2019;15(51):1906086.

[165] Liu N, Yao Y, Cha JJ, McDowell MT, Han Y, Cui Y. Functionalization of silicon nanowire surfaces with metal-organic frameworks. Nano Res 2012;5(2):109–16.

[166] Lu H, Hu R, Bai H, Chen H, Lv F, Liu L, et al. Efficient conjugated polymer–methyl viologen electron transfer system for controlled photo-driven hydrogen evolution. ACS Appl Mater Interfaces 2017;9(12):10355–9.

[167] Shan B, Brennaman MK, Troian-Gautier L, Liu Y, Nayak A, Klug CM, et al. A silicon-based heterojunction integrated with a molecular excited state in a water-splitting tandem cell. J Am Chem Soc 2019;141(26):10390–8.

[168] Zhao C. Polyoxometalates in artificial photosynthesis: Development of chromophores and water oxidation catalysts (Doctoral dissertation. Emory University; 2013.

[169] Shao Y, Xiao X, Zhu YP, Ma TY. Single-crystal cobalt phosphate nanosheets for biomimetic oxygen evolution in neutral electrolytes. Angew Chem Int Ed 2019;58(41):14599–604.

[170] Tang R, Zhou S, Yuan Z, Yin L. Metal–organic framework derived Co3O4/TiO2/Si heterostructured nanorod array photoanodes for efficient photoelectrochemical water oxidation. Adv Funct Mater 2017;27(37):1701102.

[171] Prabu S, Chiang KY. Yolk-shell silica dioxide spheres@ metal-organic framework immobilized Ni/Mo nanoparticles as an effective catalyst for formic acid dehydrogenation at low temperature. J Colloid Interface Sci 2021;604:584–95.

[172] Ball B, Chakravarty C, Sarkar P. Silicon and phosphorus co-doped bipyridine-linked covalent triazine framework as a promising metal-free catalyst for hydrogen evolution reaction: a theoretical investigation. J Phys Chem Lett 2020;11(4):1542–9.

[173] Yuan HC, Yost VE, Page MR, Stradins P, Meier DL, Branz HM. Efficient black silicon solar cell with a density-graded nanoporous surface: optical properties, performance limitations, and design rules. Appl Phys Lett 2009;95(12):123501.

[174] Yuan L, Lou M, Clark BD, Lou M, Zhou L, Tian S, et al. Morphology-dependent reactivity of a plasmonic photocatalyst. ACS Nano 2020;14(9):12054–63.

[175] Railey P, Song Y, Liu T, Li Y. Metal organic frameworks with immobilized nanoparticles: synthesis and applications in photocatalytic hydrogen generation and energy storage. Mater Res Bull 2017;96:385–94.

[176] Lei Q, Guo J, Kong F, Cao J, Wang L, Zhu W, et al. Bioinspired cell silicification: from extracellular to intracellular. J Am Chem Soc 2021;143(17):6305–22.

[177] Lebeau B, Innocenzi P. Hybrid materials for optics and photonics. Chem Soc Rev 2011;40(2):886–906.

[178] Chen F, Zhu Q, Wang Y, Cui W, Su X, Li Y. Efficient photoelectrochemical hydrogen evolution on silicon photocathodes interfaced with nanostructured NiP2 cocatalyst films. ACS Appl Mater Interfaces 2016;8(45):31025–31.